POS502 Cruise Report

R.V. Poseidon Cruise No.: 502

Dates, Ports: 15.07.2016 (Reykjavik) – 29.07.2016 (Reykjavik)

Research subject: North Kolbeinsey Ridge – volcanology and geochemistry

Chief Scientist: Dr. Isobel A. Yeo, GEOMAR, Kiel

Number of Scientists: 11

Project: NKR-Cycles

Alphabetical List of Participating Scientists

Name	Affiliation
Nico Augustin	GEOMAR, Kiel
Matthias Bodendorfer	GEOMAR, Kiel
Bryndís Brandsdóttir	University of Iceland
Patrick Cuno	GEOMAR, Kiel
Colin Devey	GEOMAR, Kiel
Lynne Elkins	University of Nebraska-Lincoln
Jan Hennke	GEOMAR, Kiel
Hannes Huusmann	GEOMAR, Kiel
Tom Kwasnitchka	GEOMAR, Kiel
Martin Pieper	GEOMAR, Kiel
Isobel Yeo	GEOMAR, Kiel

POS502 Science Party - from left to right: Isobel Yeo, Bryndís Brandsdóttir, Matthias Bodendorfer, Lynne Elkins, Jan Hennke, Patrick Cuno, Hannes Huusmann, Martin Pieper, Tom Kwasnitschka, Nico Augustin, Colin Devey

Contents

1. Acknowledgements

We would like to acknowledge Captain Matthias Günther, of the R.V. Poseidon and his Officers and Crew for their dedication and professionalism, without which this cruise would not have been possible. We thank Dr. E. Baker, Dr. S. Walker and the NOAA Vents program for the loan of the MAPR used during this expedition. We extend our gratitude to the Danish, Icelandic and Norwegian authorities for permission to work in their waters.

2. Introduction (Yeo)

Plate accretion at mid-ocean ridges is thought to be characterized by cyclic bouts of intense magmatic extrusion and intrusion separated by periods when tectonic activity accounts for plate separation. It is not known whether there is any distinct periodicity to these cycles, although the repeat rate of volcanism might be expected to be a direct function of spreading rate and an inverse function of average eruption volume. It is also unclear whether whole regions of the ridge axis have synchronized cycles. Yet eruption frequencies have direct consequences, for example, for hydrothermal mineral accumulation and chemosynthetic biodiversity, as time-between-eruption is directly linked to how long individual hydrothermal sites could be active before being covered by new lava. Based on high-resolution acoustic backscatter data from the North Kolbeinsey Ridge, a shallow slow-spreading ridge where high glacial and post-glacial sedimentation rates allow relative flow ages to be determined, we have identified several groups of possibly contemporaneous lava flows in the ridge axis using backscatter intensity as a proxy for sediment thickness and hence age.

The goal of this cruise is to sample these flows to provide samples for geochemical and geochronological studies to determine whether the flows all erupted at the same time, whether they were fed by the same source or even same magma chamber and to look at the variations in source composition through time. Additionally we aim to use photogrammetric reconstructions of the seafloor to study the detailed morphology and morphological variations of seafloor lava flows and their effect on the hydroacoustic properties. By doing this we hope to calibrate the theoretical dating done using backscatter intensity and allow this method to be applied more broadly to sidescan sonar data collected elsewhere. If successful this method will make it possible to distinguish the detailed stratigraphy of seafloor lava flows over broad areas without the need for sampling.

3. Background (Yeo, Devey, Brandsdóttir)

3.1 The Kolbeinsey Ridge

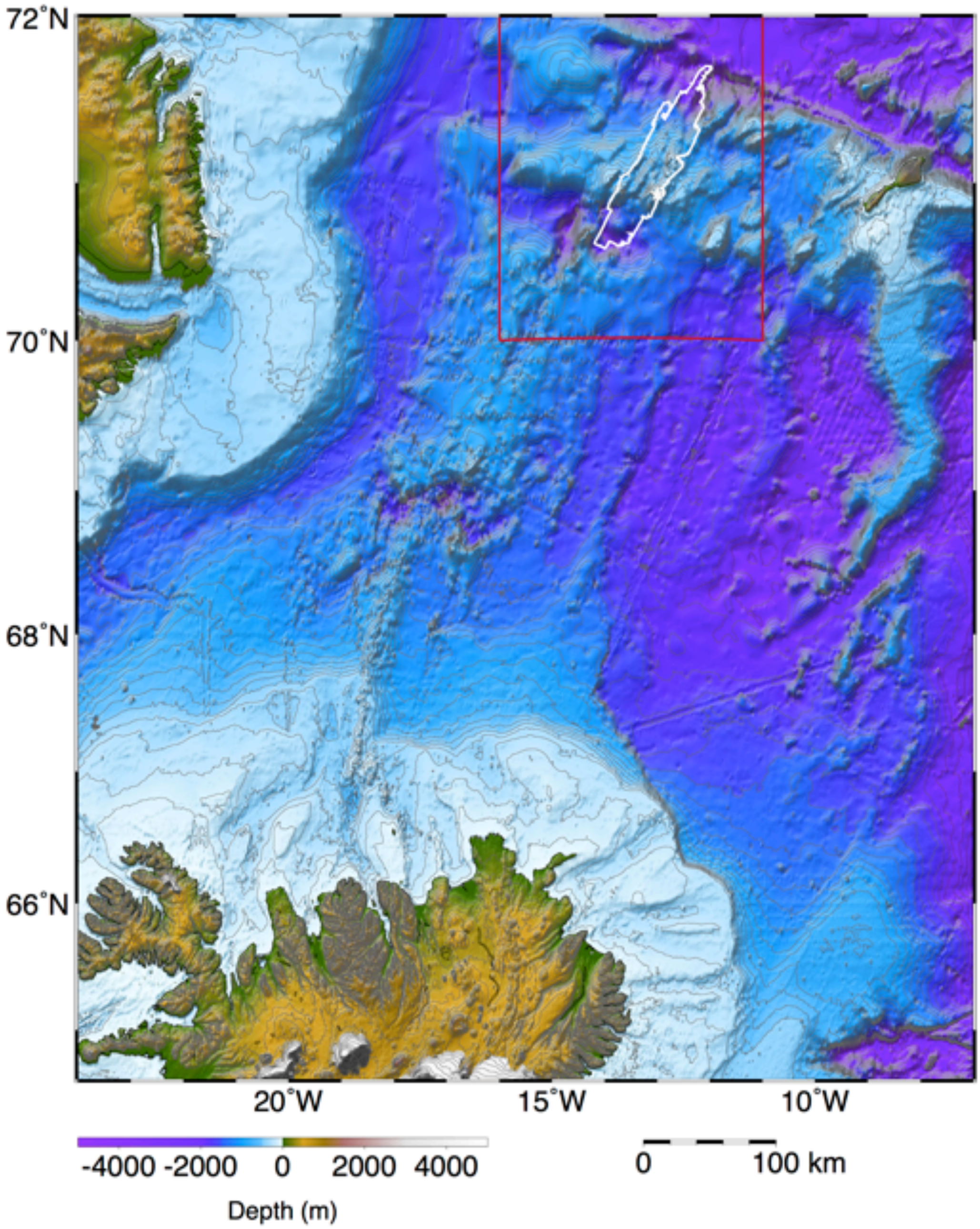

Fig. 3.1: The entire Kolbeinsey Ridge showing in the Sandwell and Smith (2014) bathymetry. The red square defines the absolute extent of the NKR. The white line shows the outline of bathymetry collected during cruise POS436 in 2012. Eggvin Bank Volcano is shown by the white star.

The Kolbeinsey Ridge spreading axis (Fig. 3.1) lies between Iceland and the Jan Mayen Fracture Zone in the arctic North Atlantic. The ridge shows anomalously shallow bathymetry along its whole length, thought to be the result of the influence of the Iceland plume leading to excessive melting and an abnormally thickened crust (e.g., Kodaira et al., 1997). The influence of the Iceland and/or Jan Mayen plumes on the axial basalts has been demonstrated geochemically (e.g., Blichert-Toft et al., 2005; Mertz et al., 2004).

The spreading axis itself can be divided into three second-order segments ("North", "Central" and "South") separated by non-transform offsets with overlapping spreading centres (e.g. Appelgate 1997). The North Kolbeinsey Ridge (NKR) stretches from 70.5ºN to 71.7ºN and shows a full spreading rate of 18 mm/yr (Mosar et al., 2002). The measured depths of the NKR spreading axis range from ca. 2500 m at the northern (adjacent to the Jan Mayen fracture Zone) and southern (adjacent to the overlapping boundary to the Central Kolbeinsey Ridge) ends to 800 m in the centre. The seafloor surrounding the axis is also characterized by generally shallow water depths that extend as far East as Jan Mayen island (and include the region known as Eggvin Bank, with water depths as shallow as 20-30m) and West towards the Greenland continental shelf (Mertz et al., 2004). Numerous authors have argued for a continental fragment underlying the island of Jan Mayen (e.g., Kandilarov et al., 2012) although geochemical work on the basalts from the NKR spreading axis itself shows no signs of a continental signature in, for example, the magmatic Ce/Pb or Nb/U values (Blichert-Toft et al., 2005). The axial basalts appear to be derived from a mantle with similar temperatures to that found beneath other, deeper regions of the Kolbeinsey Ridge, but with higher water and lower Fe contents (Haase et al., 2003). It is these lower Fe contents, which, the latter authors concluded, led to the mantle under the NKR being less dense than elsewhere and hence yielding the shallow axial depths.

Eggvin Bank volcano (Fig. 3.1) is the tallest feature on the segment (with a water depth of only 25 m at the summit) and lies on the intersection of two normal faults. Trace element measurements (Elkins et al., 2016.) from a single dredge on Eggvin bank volcano, showed they were more enriched in incompatible elements (La/Sm_N = 2.1-2.3, Sm/Yb_N = 1.2-1.3) than the surrounding NKR (La/Sm_N = 1.6-1.9, Sm/Yb_N = 0.9). This enrichment is approaching Jan Mayen Island basalt enrichment (La/Sm_N= 4.3, Sm/Yb_N = 3.8) suggesting high magma flux to Mt. Eggvin is likely the result of mantle mixing with an increased magma supply from neighbouring hotspot, Jan Mayen Island. No information is available on the stability of this process through time although a shallower off-axis trace is observable in the GEBCO 2008 bathymetry.

The Kolbeinsey Ridge is characterized by lower seismicity than the Reykjanes Ridge, south of Iceland, a pattern possibly consistent with the asymmetry in plume-ridge interaction that has been inferred from the axial depth and geochemistry of these ridges. Based on seismic data from 1970 (Fig 3.2) acquired by the National Earthquake Information System (NEIS) and Global Centroid Moment Tensor Project (GCMT), the seismicity within individual segments is highly variable (Fig. 3.2). The KR fracture zones are clearly expressed by enhanced seismicity compared to the ridge segments, with strike slip focal solutions, whereas normal faulting earthquakes, representing extension, characterize the ridge segments. A scatter of earthquakes larger than MW4 delineates the southernmost segment of the KR. The most prominent seismicity occurred at the both ends of the segment whereas the centre, at the northern margin of the Iceland Shelf, has fewer events. The northern part of the middle segment exhibits higher seismic activity compared to its southern part, whereas the northernmost segment has seemingly higher activity in its southern part.

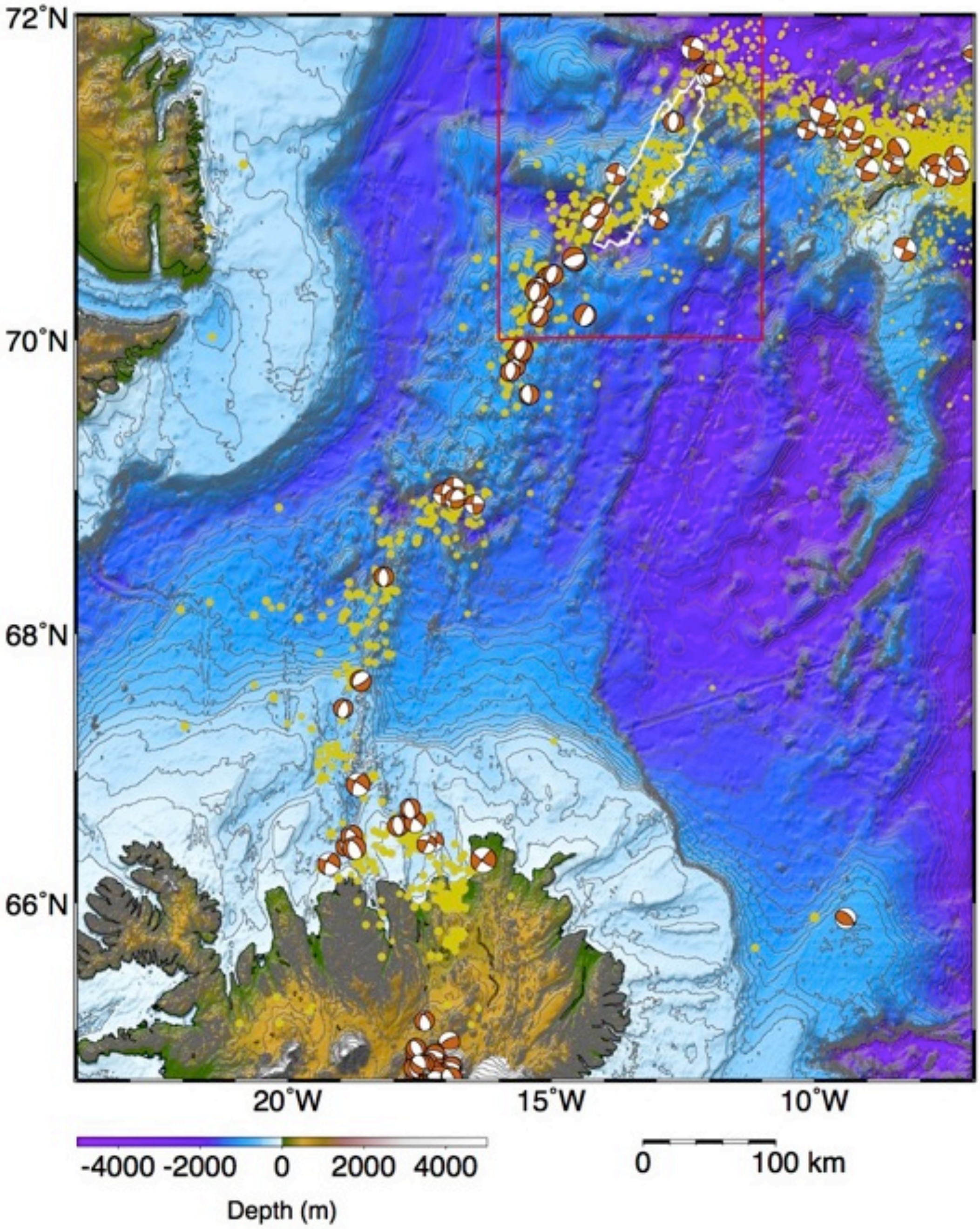

Fig.3.2: As Fig. 3.1 but showing the earthquake epicentres and centroid-moment tensor solutions from the IRIS/GCMT database spanning the 1970-2016 period (Trabant et al., 2012; Dziewonski et al., 1981, Ekström et al., 2012)

3.2 Cruise POS436 (2012)

Over 80% of the NKR neovolcanic zone was surveyed in 2012 using a ship-mounted multibeam system during POS436 (Devey et al., 2012; Yeo et al., 2016). The geological map produced shows the structure of the NKR ridge axis to be relatively simple in the north, characterized by a normal-fault-bounded axial valley containing numerous flat-topped seamounts. The centre of the segment is dominated by the Eggvin Bank volcano and comprises mostly smooth, occasionally cratered, terrain with very few flat-topped seamounts or hummocky lava flows. This smooth terrain appears to be the dominant product of volcanic activity across the shallow central part of the segment, suggesting that much of the seafloor is covered by low relief sheet or lobate flows interspersed with spatially limited areas of hummocky volcanic terrain. This relative distribution of volcanic terrain types is different to that typically observed on slow-spreading ridges, which tend to comprise a higher percentage of hummocky volcanics (e.g. Smith and Cann, 1990). The southern end of the NKR is much more complicated, with two volcanic zones separated by a 10 km wide sliver of tectonised, probably older seafloor. This area is interpreted as an overlap zone between the Northern and Middle Kolbeinsey Ridge, with the oblique section of the valley between 70º50 and 70º57 bound by oblique faults that accommodate this overlapping.

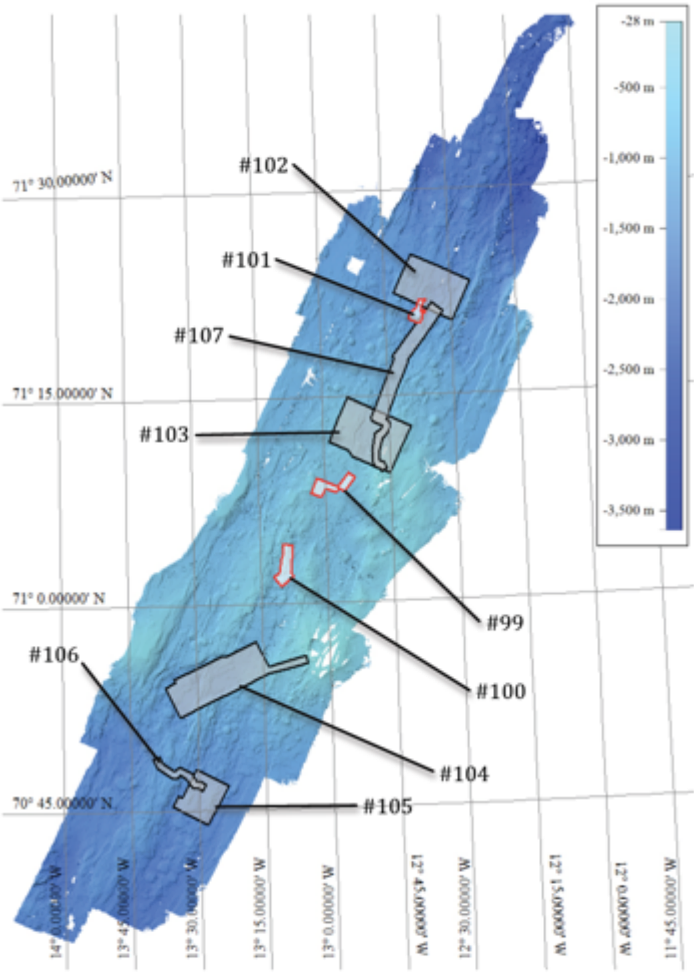

Fig. 3.3 Bathymetry from POS436 in 2012 showing the areas of sidescan sonar AUV surveys (black outlines) and high-resolution multibeam bathymetry (red outlines).

Several areas of the ridge were surveyed in high-resolution (2 m) by the GEOMAR AUV Abyss using a 120 kHz sidescan sonar system. Numerous dredge samples were also collected on and to either side of the ridge axis and on the Eggvin Bank Volcano. Further volcanic wax corer samples were collected in high-density on a single flat-topped seamount at the northern end of the NKR. MAPR were deployed on all sampling equipment but returned little evidence of hydrothermal activity. The bathymetry collected during POS436 and the AUV deployment areas are shown in Fig. 3.3.

3.3 Volcanism at Slow-Spreading Mid-Ocean Ridges

Volcanic activity even at the most fast-spreading ridges is not continuous in nature, but consists of short periods of eruption/intrusion punctuated by long periods of volcanic quiescence, during which tectonic activity is thought to account for the plate movement. This interplay between volcanism and tectonism may, at fast-spreading ridges at least, play a major role in how Layer 2A of the oceanic crust grows (Escartín et al., 2007) and on the global MOR system may control both the fractionation state and the degree of source heterogeneity shown by the erupted lavas (Rubin and Sinton, 2007). Attempts to place an age-scale on the cyclicity at fast-spreading ridges have shown little success (e.g. Bowles et al., 2006) probably due to the extremely high-frequency of eruptions there.

Evidence for such volcano-tectonic cycles on slow- and ultraslow-spreading mid-ocean ridges is also well documented. More irregular melt supply as a result of the slower spreading rate suggests that periods of high-magmatic activity followed by periods of quiescence and tectonic extension may be necessary to form Axial Volcanic Ridges (AVRs) and account for ridge segments which show large degrees of tectonic degradation with little apparent recent volcanism (Parson et al., 1993) (Fig. 3.4). Estimates of cycle lengths in the literature are highly variable ranging from several hundreds of thousands of years, based on seafloor morphology (Searle et al., 1998; Mendel et al., 2003), to tens of thousands of years based on direct seafloor observation and seismic studies of magma chamber volume beneath the southern Reykjanes Ridge (Bryan and Moore, 1977; Sinha et al., 1998; Ballard and Van Andel, 1977). More recently Searle et al. (2010) and Yeo and Searle (2012) present data suggesting almost all the lavas within the axial valley of the MAR at 45ºN are less than 50ka, however, relatively few samples are analysed in this study, no specific lava flows are identified and no higher resolution dates are available.

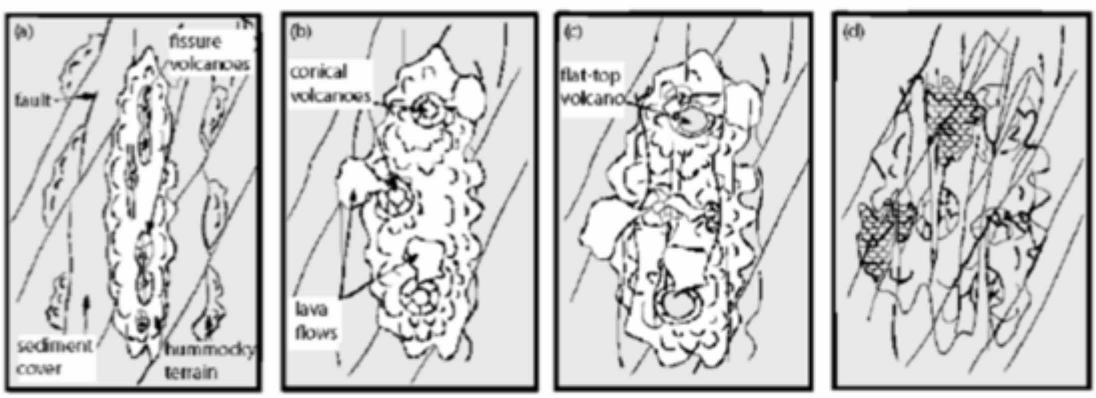

Fig. 3.4: Life cycle model for slow-spreading Mid-Ocean Ridge from Pierce et al. (2005) adapted from Parson et al. (1993).

3.4 Dating Mid-Ocean Ridge Lava Flows using Hydroacoustic Measurements

Dating young basalts accurately is notoriously difficult yet essential if we are to reconstruct volcanic histories and understand volcanic/tectonic cycles on mid-ocean ridges. There are very few mid-ocean ridges for which we have any knowledge of the eruption history over a relevant period of time. Individual lava flow fields have been successfully mapped and measured using repeat bathymetric surveying (Caress et al., 2012; Fox et al., 1992), but radiometric dating of these flows (e.g. Duncan and Hogan, 1994) and reconstruction of geological histories is commonly limited by the sample density. Others have used sediment drape thickness as a proxy for age (Mitchell, 1993, 1995a) using data from both sub-bottom profilers and sidescan sonar to differentiate relatively large differences in drape thickness. Paleomagnetic studies have also provided useful age information (e.g. Schouten et al., 1999), but require near bottom magnetometer surveys, while some successful work has been done using geomagnetic paleointensity of submarine basaltic glasses (Bowles et al., 2005).

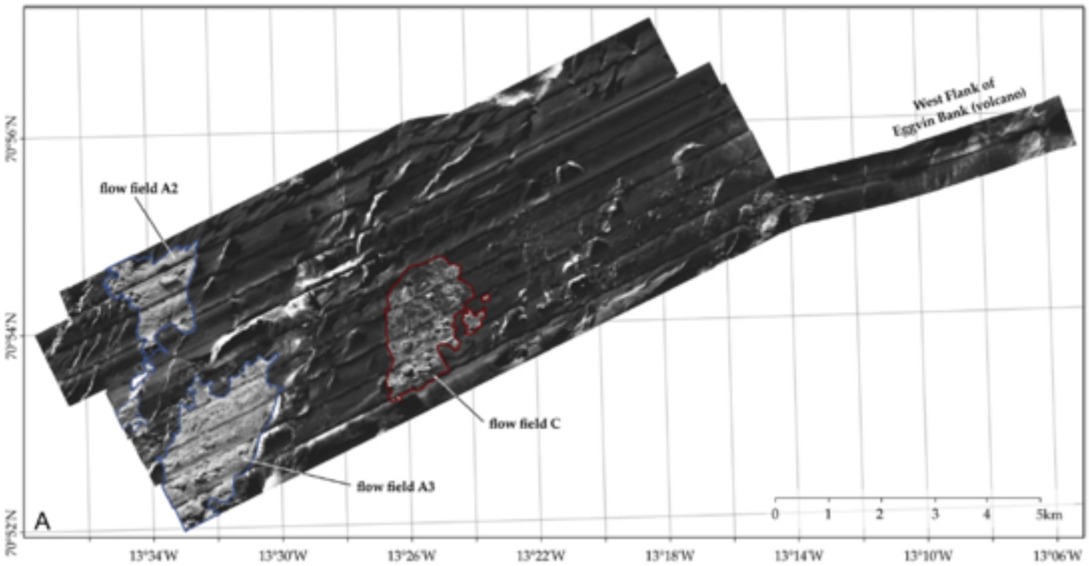

Fig. 3.5: Three lava flows in the oblique valley area of the NKR imaged in a single AUV Abyss sidescan sonar dive in 2012. The two flows with the blue outlines are more brightly and uniformly backscattering than the flow outlined in red, which we believe to be older.

Deep submergence, high-frequency sidescan sonar has, in regions with well constrained sedimentation rates, the potential to simultaneously yield information on both flow field ages and their areal extents and distribution. During the 2012 expedition to the NKR 6 areas of the ridge axis (with a combined area of >150 km2) were imaged using the 120 kHz sidescan sonar on the AUV Abyss. Of these areas 60% of the seafloor showed low and featureless acoustic backscatter, with no signs of recent volcanic activity. Based on the attenuation coefficient of deep seafloor sediment these areas are likely covered with >2m of sediment. The remaining 40% of the surveyed area showed high-backscatter smooth terrain (e.g. Fig. 3.5). This terrain could be further subdivided, based on its backscatter signals, into 16 lava flows varying in area between 0.3 km^2 and 15.8 km^2. Using the differences in amplitude between the different flows, these backscatter variations could be turned into estimates of the relative sediment cover thicknesses (and therefore age) of the flows. Of the dated flow fields, none appear to be older than 3.2 ka and a group appear to have erupted within 1000 years of each other. (Yeo et al., 2016). However, this method involves many assumptions and has never been tested with visual observations of the surveyed seafloor.

3.5 POS502

During POS502 detailed photogrammatrical reconstructions of the seafloor with the DeepSurveyCam System (mounted on the ROV PHOCA) will allow for the sediment thickness to be accurately measured in order to ground truth the theoretical method. These reconstructions will also be used to assess the detailed effect seafloor geometry and variable seafloor properties can have on hydroacoustic returns. By providing accurate dates for seafloor lava flows we hope to better understand the frequency, style and extent of lava flows, and by providing quantitative constrains on the theoretical ages calculated using backscatter intensity we aim to test and calibrate the method so that it can be used elsewhere and applied to older datasets.

The Wax Corer sampling program will sample all the flows that were mapped and dated using the backscatter method. Major and trace element analyses of these samples back on land will allow us to test whether lava flows the same/similar ages are fed by the same source or from discrete magma bodies. We will also densely sample some of the lava flows to assess the changing chemistry of a mid-ocean ridge eruption over time. By sampling vents, distal areas and differing flow textures in between we aim to build a detailed geochemical model of the magma chemistry throughout the course of a single eruption. We will also attempt to sample along possible dyke pathways to see if evidence for magma propagation away from a central source can be observed.

Dredging will be attempted on off axis Eggvin Bank Volcano to establish the longevity and geochemical history of this anomalously shallow terrain.

4. Cruise Narrative (Yeo)

4.1 Daily Narrative

15.07.2016
Following mobilisation of the ROV and a successful harbour test on the 14.07.2016 we sent sail promptly at 09:00 on the 15.07.2016 towards our first survey area on the Southern Kolbeinsey Ridge.

16.07.2016
Some rougher weather north of Iceland slowed our progress a little, however, the weather improved in the evening and overnight meaning only a few hours were added to the transit time.

17.07.2016
Better weather overnight got us on station for the first multibeam survey on Southern Stóragrunn , Southern Kolbeinsey by 00:30. The tracks covered volcanic terrain surveyed periodically by Icelandic expeditions looking for young volcanic activity. The data collected covered 9.5 km^2, however, comparison with data collected in 2002 showed no evidence for major volcanic activity in the last 14 years. With the survey completed we continued our transit to Northern Kolbeinsey.

18.07.2016
We arrived in the main working area at 02:30 and surveyed a multibeam line into the survey area to check the positioning of the bathymetry collected in 2012. We then conducted two successful Volcanic Wax Corer deployments in the south of the working area. Both brought back very fresh looking glassy chips from a young lava flow mapped using the 2012 AUV data. We followed this with a fascinating ROV dive over the lava flows we had just sampled with the Deep Survey Cam system. Many different lava flow contacts were observed, along with several patches of hydrothermally altered sediment and interesting tectonic features.

19.07.2016
In the morning we mapped westwards from the centre of the parallel valleys to the south of the NKR across what appears to be an overlapping spreading centre with the Middle Kolbeinsey (MKR). The survey revealed the NKR and the MKR are separated by a 1000m faulted-high and revealed some old volcanic material at the northern end of the MKR at a similar latitude to that which volcanic features stop being visible on the NKR.

20.07.2016
We started the day by successfully sampling the southern of the two flows in the eastern of the two parallel valleys. We then travelled north to the oblique valley that connects them to the main ridge for an ROV dive. The ROV observations matched well with the AUV Sidescan Sonar, revealing an older, sedimented lava flow as predicted from the backscatter intensity. We then did a blue jump across to a younger looking flow in the AUV data which turned out to be composed of young looking pillow lavas and almost completely unsedimented whorly and

hackly fissured sheet flows. Overnight we continued to map the southern end of the segment with the ship system, revealing an interesting intersection of the eastern valley with the western one.

21.07.2016
A very quick ROV dive revealed young pillow lavas on a young lava flow in the centre of the segment identified in the AUV sidescan data . Sampling targeted the same lava flow and one similar looking flow to the north successfully. Over night we surveyed the crater off Eggvin volcano and the volcano off axis with the ship multibeam system.

22.07.2016
Twelve wax corer deployments, of which 11 returned samples, were conducted over the central NKR. These locations targeted several lava flow fields mapped as different as well as specific features, including likely vent structures, morphological changes and distal ends of likely flows. Multibeam surveys with the ship overnight extended the surveyed area to the east revealing older faulted terrain and old volcanic features.

23.07.2016
Two dredges in the morning successfully recovered samples from off axis Eggvin volcano and from the volcano crater, including vesicular samples that popped on deck. A short ROV dive in the afternoon inside the active Eggvin Bank Volcano crater covered young looking cones inside the crater and found very young looking rocks, corresponding to the dredge track and several sites of hydrothermal venting that were both observed in the video and picked up in the redox potential measurements of the MAPR (Miniature Autonomous Plume Recorder) mounted on the vehicle. Multibeam overnight extended the survey off Eggvin Bank Volcano further to the east.

24.07.2016
A morning ROV dive covered a lava flow field in the central NKR over numerous lava flow morphologies, including large areas of ropy and hackly sheet flows o n the seafloor, a cratered smooth seamount and a pillow mount. Indications of hydrothermal activity were again observed, corresponding to large redox potential anomalies recorded on the MAPR. Multibeam overnight continued to extend the mapped area to the east.

25.07.2016
Two wax corers in the morning successfully recovered glass from older flows in the north of the working area. A very short ROV dive revealed the texture of a flow mapped as slightly older from the AUV data to be pillow lavas covered with a dusting of sediment. Three more wax corers in the evening allowed us to collect samples of the vent and distal areas of this flow. Multibeam overnight extended the mapped area to the southeast.

26.07.2016
As we had to leave the survey area by 17:00 we launched the ROV in the morning in order to have a more in depth look at the crater of Eggvin Volcano. The crater walls in particular involved some difficult flying for the ROV pilots and extra

effort positioning the ship, which are much appreciated. Many interesting features were observed on the crater floor and walls, including possible old hydrothermal sites and dykes cutting across the volcano. The end of the dive was located over the crater rim on the volcano flanks to the north, both here and on the crater floor the seafloor was covered by very crumbly, vesicular, dark volcanic material, likely produced by a recent volcanic eruption that postdates the crater formation. Multibeam surveys with the ship on the way out of the working area extended the mapped area south to the termination of the NKR segment and across to the overlap with the MKR.

27.07.2016

Good weather and wind from the north meant we made good progress on today's transit. The science party have continued working up their data while the ROV team have begun demobilisation of the vehicle ready for shipping in Reykjavik.

28.07.2016

The transit towards Reykjavik continued as planned. The scientists and ROV team have been busy packing up the equipment, cleaning laboratories and writing up results.

4.2 Station list

Station No.	Date	Latitude	Longitude	Equipment	Samples taken/Area surveyed
294/1	17.07.16	66° 56.17' N	018° 25.84' W	MB	Southern Stóragrunn , Southern Kolbeinsey
295/1	18.07.16	70° 07.79' N	014° 42.31' W	MB	South of mapped area
296/1	18.07.16	70° 47.04' N	013° 32.16' W	VSR	Yes - glass chips
297/1	18.07.16	70° 46.90' N	013° 30.62' W	VSR	Yes - glass chips
298/1	18.07.16	70° 47.26' N	013° 30.06' W	ROV	Young lava flow in eastern parallel valley N NKR
299/1	18.07.16	70° 44.17' N	013° 18.70' W	MB	South of mapped area
300/1	19.07.16	70° 45.65' N	013° 32.01' W	VSR	Yes - glass chips
301/1	19.07.16	70° 54.30' N	013° 26.51' W	VSR	No - mud
302/1	19.07.16	70° 49.93' N	013° 53.74' W	MB	Western side of surveyed area
303/1	20.07.16	70° 54.66' N	013° 33.00' W	VSR	Yes - glass chips
304/1	20.07.16	70° 54.28' N	013° 33.73' W	VSR	Yes - glass chips
305/1	20.07.16	70° 54.03' N	013° 33.84' W	VSR	Yes - glass chips
306/1	20.07.16	70° 52.78' N	013° 32.13' W	VSR	Yes - glass chips
307/1	20.07.16	70° 54.01' N	013° 25.94' W	VSR	Yes - glass chips
308/1	20.07.16	70° 54.07' N	013° 24.35' W	ROV	Young and older lava flows in oblique valley
309/1	20.07.16	70° 36.91' N	014° 18.51' W	MB	Along Norway/Denmark EEZ boundary
310/1	21.07.16	71° 14.62´N	012° 44.74´W	VSR	Yes - glass
311/1	21.07.16	71° 15.26´N	012° 43.91´W	VSR	Yes - small glass chips
312/1	21.07.16	71° 15.95´N	012° 42.82´W	VSR	No – only mud recovered
313/1	21.07.16	71° 16.30´N	012° 42.48´W	VSR	Yes - chips in cups, rock on side
314/1	21.07.16	71° 16.05´N	012° 43.75´W	VSR	Yes - one small piece
315/1	21.07.16	71° 16.05' N	012° 43.86' W	ROV	Young lava flow(s) in central NKR area
316/1	21.07.16	71° 16.78´N	012° 43.31´W	VSR	Yes - glass

317/1	21.07.16	70° 57.58' N	013° 05.64' W	MB	Eggvin Volcano crater and off axis
318/1	22.07.16	71° 12.26´N	012° 49.78`W	VSR	Yes - small glass & rock chips
319/1	22.07.16	71° 12.62´N	012° 49.20´W	VSR	Yes, one larger chip. Looks old
320/1	22.07.16	71° 13.07´N	012° 48.02´W	VSR	Yes, glass chips looking fresh
321/1	22.07.16	71° 13.53´N	012° 45.98´W	VSR	Yes - cups full
322/1	22.07.16	71° 13.82´N	012° 45.54´W	VSR	Yes - glass chips
323/1	22.07.16	71° 15.26´N	012° 45.64´W	VSR	Yes - glass with some mud
324/1	22.07.16	71° 15.19´N	012° 44.03´W	VSR	No – no recovery
325/1	22.07.16	71° 15.18´N	012° 44.05´W	VSR	Yes - glass with mud
326/1	22.07.16	71° 14.31´N	012° 46.87´W	VSR	Yes - v. fresh glass, little sediment
327/1	22.07.16	71° 16.10´N	012° 43.05´W	VSR	Yes - glass chips
328/1	22.07.16	71° 16.82´N	012° 43.88´W	VSR	Yes - glass
329/1	22.07.16	71° 16.84´N	012° 41.96´W	VSR	Yes – mostly mud but one rock fragment
330/1	22.07.16	71° 32.78' N	012° 28.53' W	MB	Western side of surveyed area
331/1	23.07.16	70° 54.96' N	012° 44.06' W	DR	Yes, 2 basaltic samples with glass plus dropstones
332/1	23.07.16	70° 57.05' N	013° 02.90' W	DR	Yes, numerous, vesicular basaltic samples taken
333/1	23.07.16	70° 57.04' N	013° 03.42' W	ROV	Eggvin Bank Volcano crater
334/1	23.07.16	70° 53.32' N	012° 40.81' W	MB	Western side of surveyed area
335/1	24.07.16	71° 12.03' N	012° 52.33' W	ROV	Young lava flows in central NKR area
336/1	24.07.16	71° 12.14´N	012 °50.16´W	VSR	Yes - fresh glass
337/1	24.07.16	71° 11.17´N	012 °49.68´W	VSR	Yes - mud with glass
338/1	24.07.16	70° 53.59' N	012° 59.11' W	MB	Western side of surveyed area
339/1	25.07.16	71° 22.21' N	012° 30.15' W	VSR	Yes - glass with mud
340/1	25.07.16	71° 22.87' N	012° 33.47' W	VSR	Yes - glass with mud
341/1	25.07.16	71° 22.57' N	012° 38.90' W	ROV	Young lava flows in central NKR area
342/1	25.07.16	71° 22.58' N	012° 37.95' W	VSR	Yes - glass with mud
343/1	25.07.16	71° 23.06' N	012° 34.13' W	VSR	Yes - glass with mud
344/1	25.07.16	71° 21.46' N	012° 31.63' W	VSR	Yes - glass with mud
345/1	25.07.16	71° 21.49' N	012° 31.62' W	MB	Western side of surveyed area
346/1	26.07.16	70° 56.73' N	013° 3.25' W	ROV	Eggvin Bank Volcano Crater
347/1	26.07.16	70° 57.55' N	013° 2.12' W	MB	Southern extent NKR

VSR – Volcanic Wax Corer
MB – Ship SB3100 Multibeam Echosounder System
ROV – Remotely Operated Vehicle PHOCA
DR – Chain bag dredge

4.3 Map of deployments

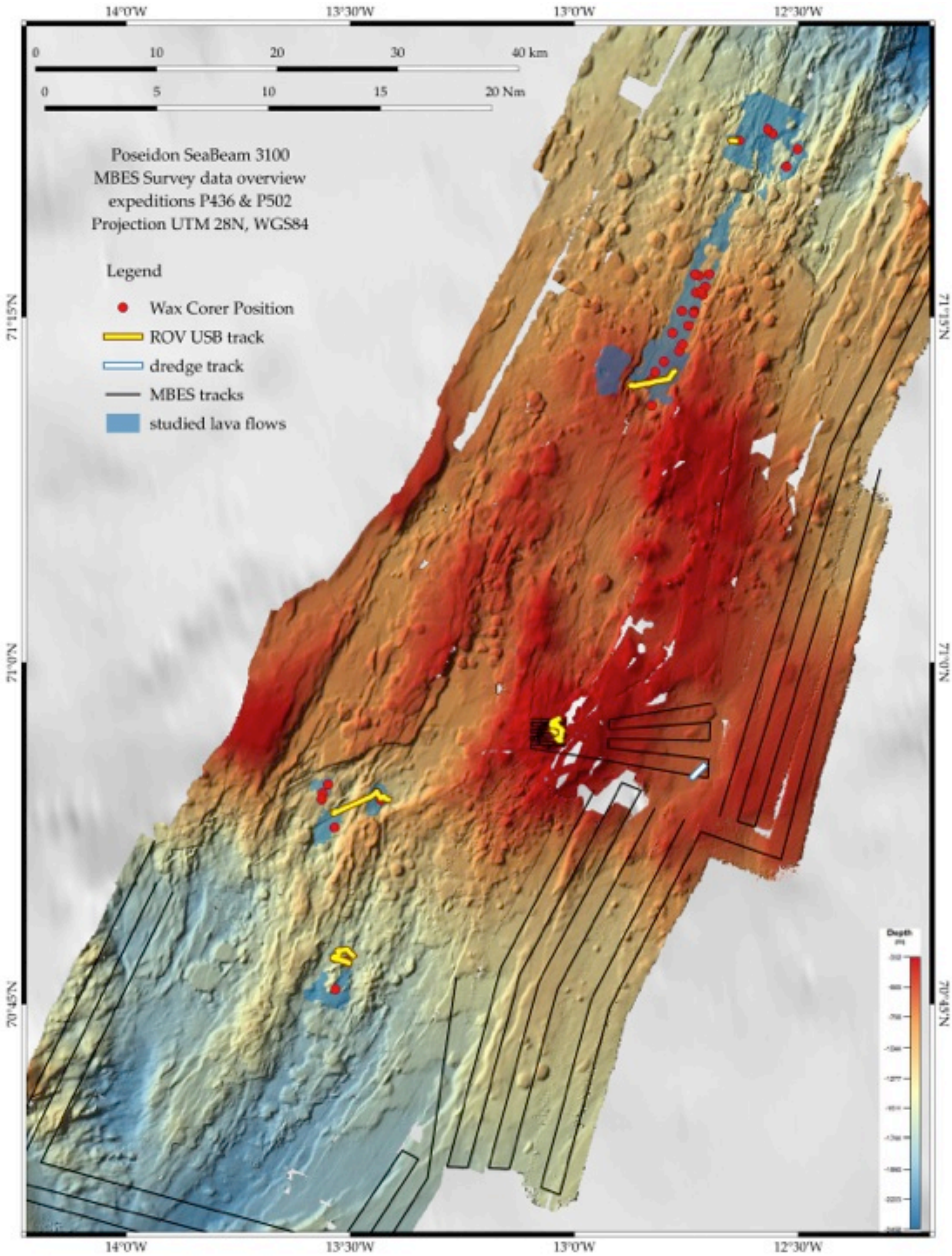

5. Bathymetry (Augustin, Brandsdóttir)

During RV Poseidon cruise P502 multibeam mapping was carried out by a Seabeam 3000 series echosounder system (SB3100) provided by ELAC Nautik GmbH. The SeaBeam 3100 multibeam echosounder (MBES) collects bathymetric, corrected backscatter, side scan and water column imaging (WCI) data at medium depths. The configuration installed on RV Poseidon operates in the 50 kHz frequency band at water depths ranging from 3 m below the transducers to approximately 3,000 m. However, beside this theoretical values we observed that the best operation depth under optimal weather conditions is between >100 m to <2000 m water depth. It has an across-ship swath width of up to 140 degrees with up to 630 beams for each multi-ping. The complete system consists of 2 transmitter/ receiver units, a motion sensor (Coda Octopus F180), and a salinometer installed on RV Poseidon. The system was operated with HydroStar v4.0. Data acquisition was performed with Hypack 14. The Hysweep survey module of Hypack bundle collected all data from the SeaBeam echo sounder in HSX data format, which was used for further processing. Since the HSX data contain all necessary information for post processing work the native ELAC XSE-data format was not stored during the cruise.

For sound velocity corrections a CTD profile, obtained during cruise P436 was used. Recent sound velocity data from ROV dives did not show any significant differences.

Before reaching the main working area at the northern Kolbeinsey Ride a small multibeam survey was carried out in the south of the Stóragrunn volcano in Icelandic waters to compare the bathymetry to seafloor data that where collected in 2002 to see if any new volcanic cones grew within the last 14 years – no significant differences were observed (Fig. 5.1).

In the main working area at the N-Kolbeinsey Ridge bathymetric mapping reached a total seafloor coverage of 22,850 km^2 mostly concentrated to extend the dataset from P436 towards the South and East as well as to collect high resolution data of the Mt. Eggvin caldera (Fig. 5.2). The reported issues with the RV Poseidon multibeam data from P436 in 2012 lead to an extensive renavigation of this data. Therefore, P502-MBES data, crossing known terrain from P502, were used to check the positioning accuracy and positioning of the 60 m P436-grid that could be verified. No significant shifts or offsets could be reported but a few, minor differences in feature geometry (a result of the renavigation procedure) were obvious.

The recorded HSX raw data were copied and (preliminary) post processing was done with QPS Qimera (Version 1.2.5, Mac). Maps were created with Global Mapper 16 and QGIS 2.14 (Essen). Preliminary grids yielded a spatial resolution of 40 m for the deeper areas and up to 10 m cell size for the Eggvin caldera (Fig. 5.3). However, final data processing and gridding will be done after the expedition at GEOMAR, Kiel. The data will be also stored at GEOMAR, Kiel for scientific use and become public available via the Pangaea scientific data repository (pangaea.de) at a later stage.

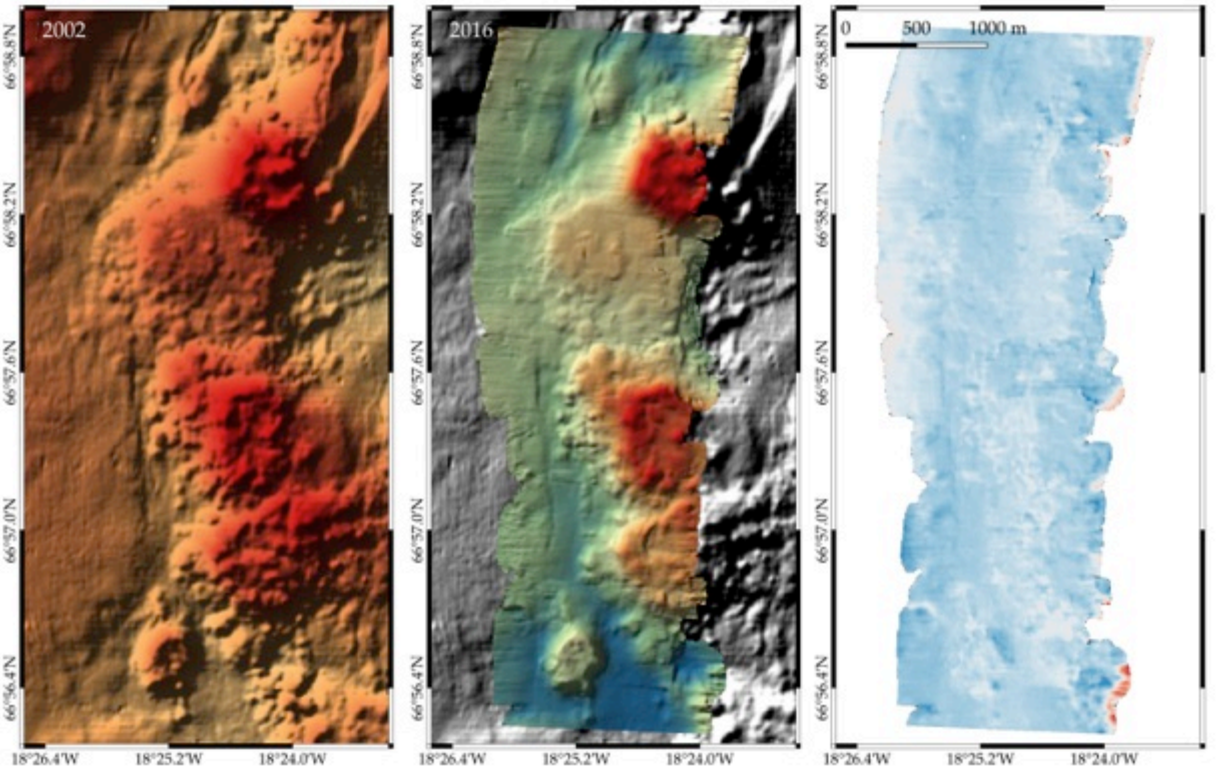

Fig. 5.1: Comparison of the bathymetric datasets of the volcanic field south of Stóragrunn Volcano (Iceland). Left: the data collected in 2002. Middle: The 2002 data (grey) overlain by the 2016 data. Right: comparison of the grids (light blue areas mark no significant variation (± a few meters only), dark blue and red mark areas with negative or positive or offset, respectively). The maximum offset of the new grid is about +20m in the SE-corner, which is due to outer beam quality but within the expected error margin.

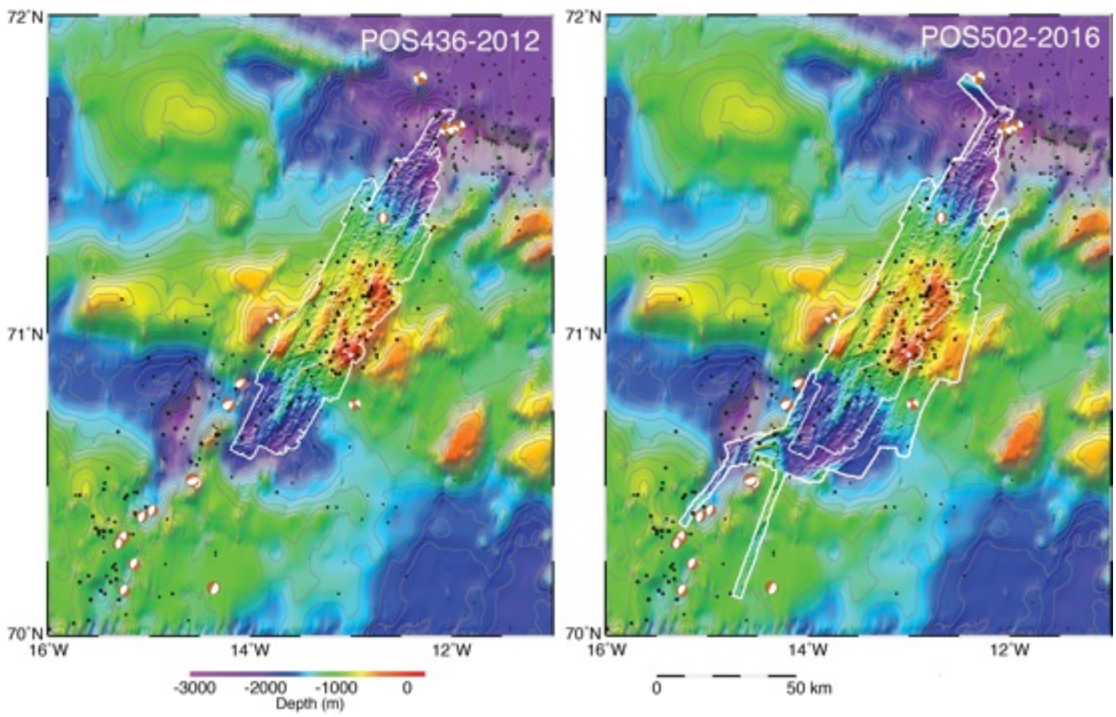

Fig. 5.2 The areas covered in 2012 and 2016 shown with the earthquake locations and moment-tensor locations.

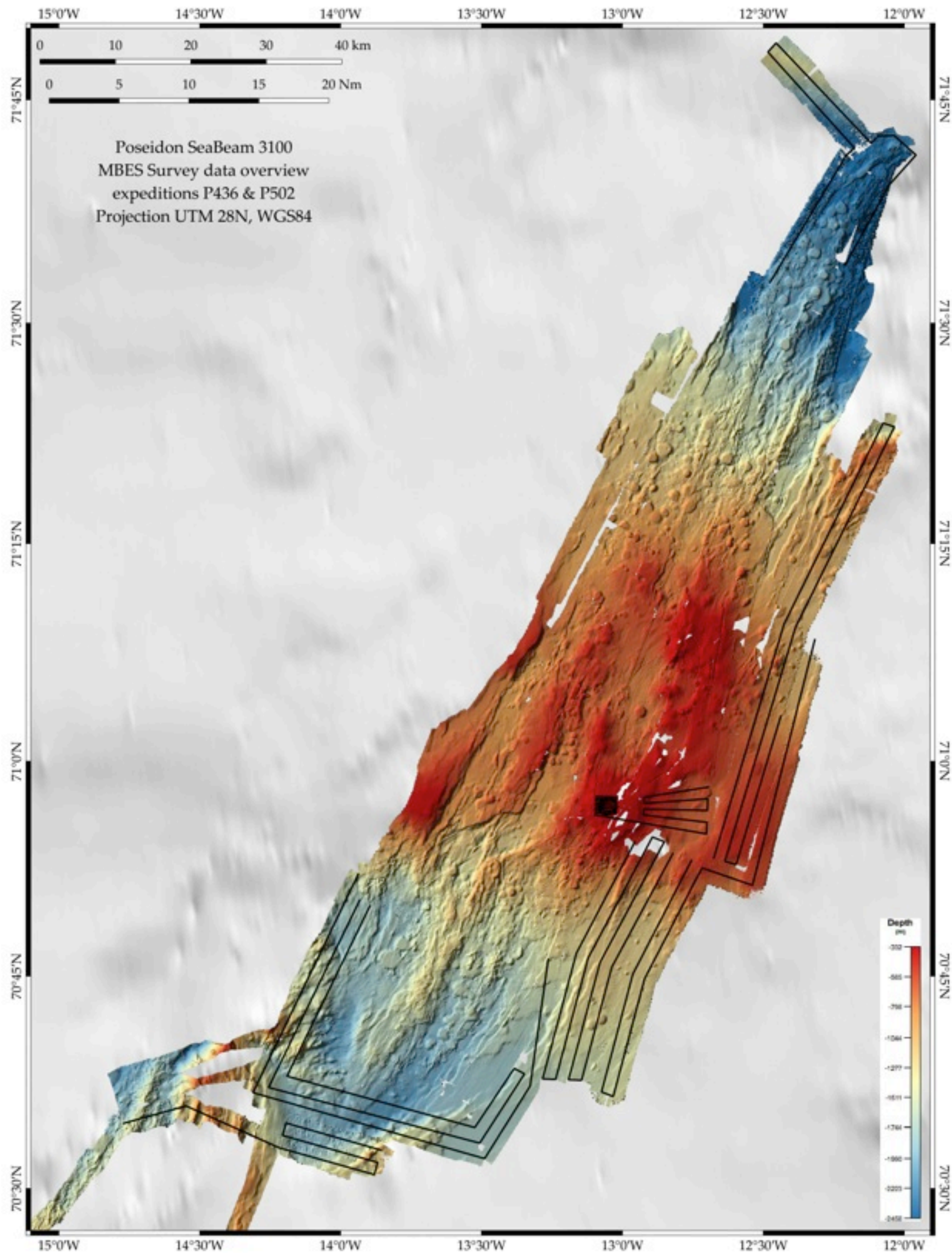

Fig. 5.3: Overview of the P436 (2012) and P502 (2016) data. The black lines represent the planned survey lines, showing the focus of the MBES surveys to extend the bathymetric dataset towards the southern end of the NKR segment, east of the 2012 dataset as well as the Eggvin caldera.

6. ROV Deployments (Yeo, Pieper, Bodendorfer, Cuno, Hennke, Huusmann)

6.1 ROV PHOCA

The *ROV PHOCA* (Fig. 6.1) is a 3000 m rated deep diving platform manufactured by SubAtlantic FET, Aberdeen, Scotland. It is based on commercially available ROVs, but customized to our demands, e.g. being truly mobile. As an electric work class ROV of the type Comanche, this is build No. 21. ROV PHOCA is based at the Helmholtz Centre for Marine Sciences GEOMAR in Kiel, Germany. During POS502 a mid-water a steel armoured, fibre optic cable was used with a maximum length of 2700 m and a 19 mm diameter. The vehicle carries various cameras: 1 HDTV Bullshark (which was not recorded all the time), 2 colour-zoom video cameras (OE14-366) mounted on pan and tilt units, one black and white video camera (OE15-108) and a digital stills camera. In addition to these cameras the vehicle was also carrying the GEOMAR DeepSurveyCam system (details can be found in section X). Lighting for the video cameras was provided by 4 Multi-SeaLite Matrix LEDs (250 W) and 4 dimmable 250 W Deep Multi-SeaLite halogen lights, the DeepSeaCam flash was provided by 2 high power LED strobe arrays, held in the vehicle's manipulator arms.

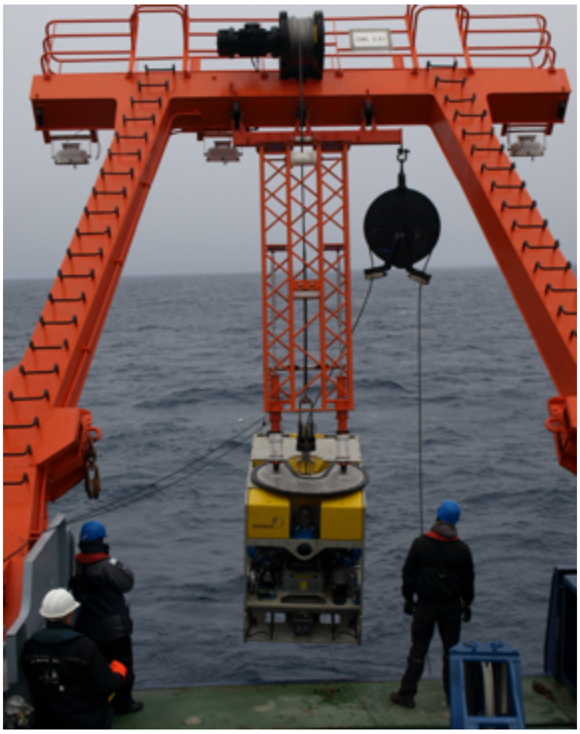

Fig. 6.1: ROV PHOCA being deployed using the LARS mounted on the A-Frame

Navigation was provided by two ORE Trackpoint USBL-Transponders (Sonadyne) communicating to a transducer deployed through the ship moonpool, with a CDL TOGS fiberopics Gyro and an RD Instruments 1200 Doppler Velocity Log. The vehicle also carried a FastCAT CTD SBE 49 manufactured by Sea-Bird and a Miniature Autonomous Plume Recorder (MAPR) mounted on the frame. Real time observational logs were kept using OFOS (Ocean Floor Observation System) by a scientist in the laboratory.

6.2 ROV PHOCA Mission Summaries

Station Number:	298-ROV			
Cruise Number:	POS502	**Equipment:**		
Date:	18.07.2016		DeepSurveyCam	
Time in Water:	13:21	**Issues:**	Slightly noisy nav	
Time on Bottom:	14:22		Tether twisted on recovery and damaged	
Time off Bottom:	20:10			
Time out of Water:	21:01			
Total Dive Time:	07:40			
Total Bottom Time:	05:47			
Distance Covered:	4.2 km	**Lat/Lon**	70° 47.26	- 013° 30.06

Dive Map:

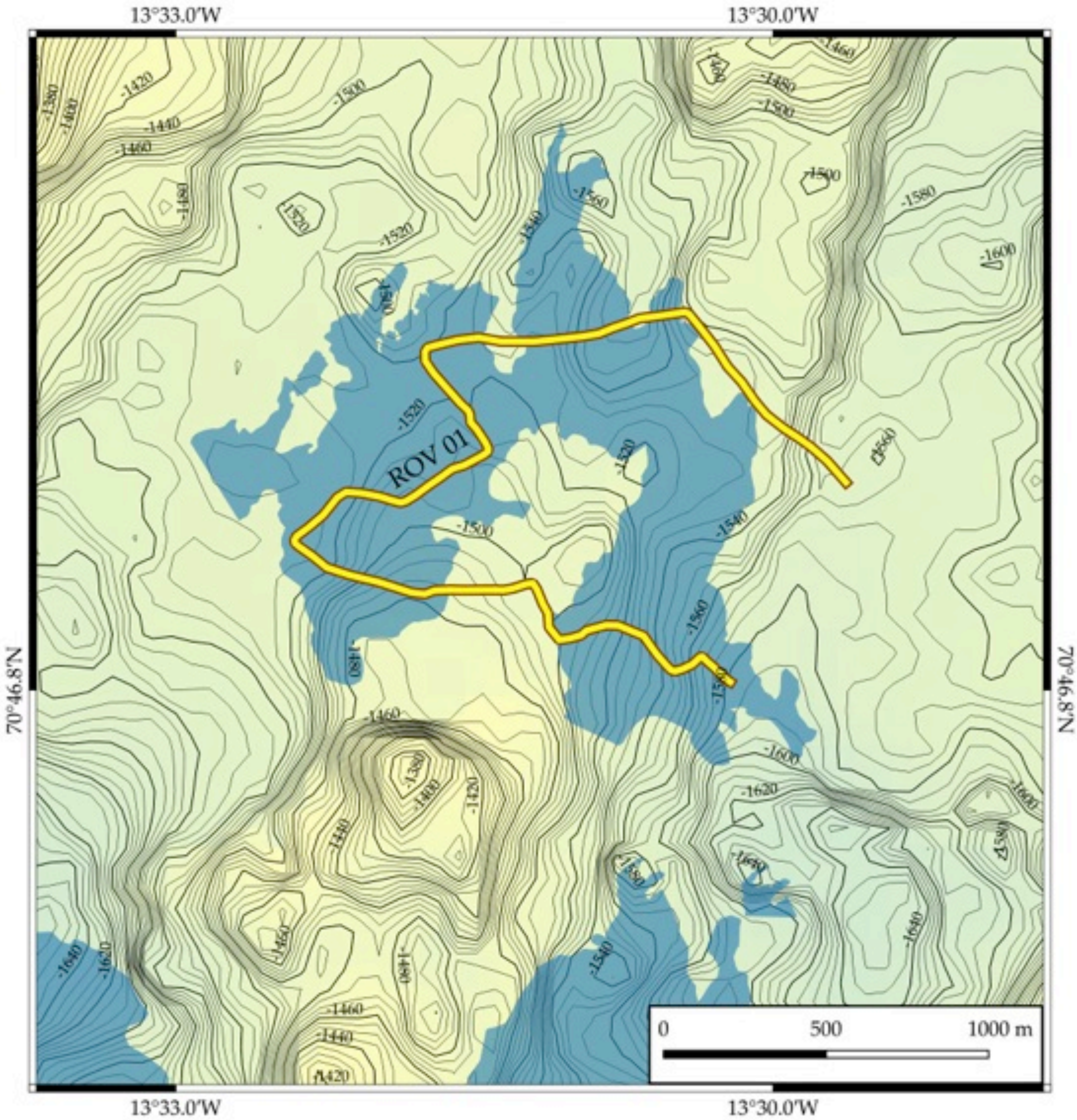

Notes:	Young pillow lavas observed and clear contacts with older sedimented areas

Station Number:	308-ROV		
Cruise Number:	POS502	**Equipment:**	DeepSurveyCam
Date:	20.07.2016		
Time in Water:	13:23	**Issues:**	Slightly noisy nav
Time on Bottom:	14:05		
Time off Bottom:	19:38		
Time out of Water:	20:25		
Total Dive Time:	07:02		
Total Bottom Time:	05:33		
Distance Covered:	5.6 km	**Lat/Lon**	70° 54.07 / - 013° 24.35

Dive Map:

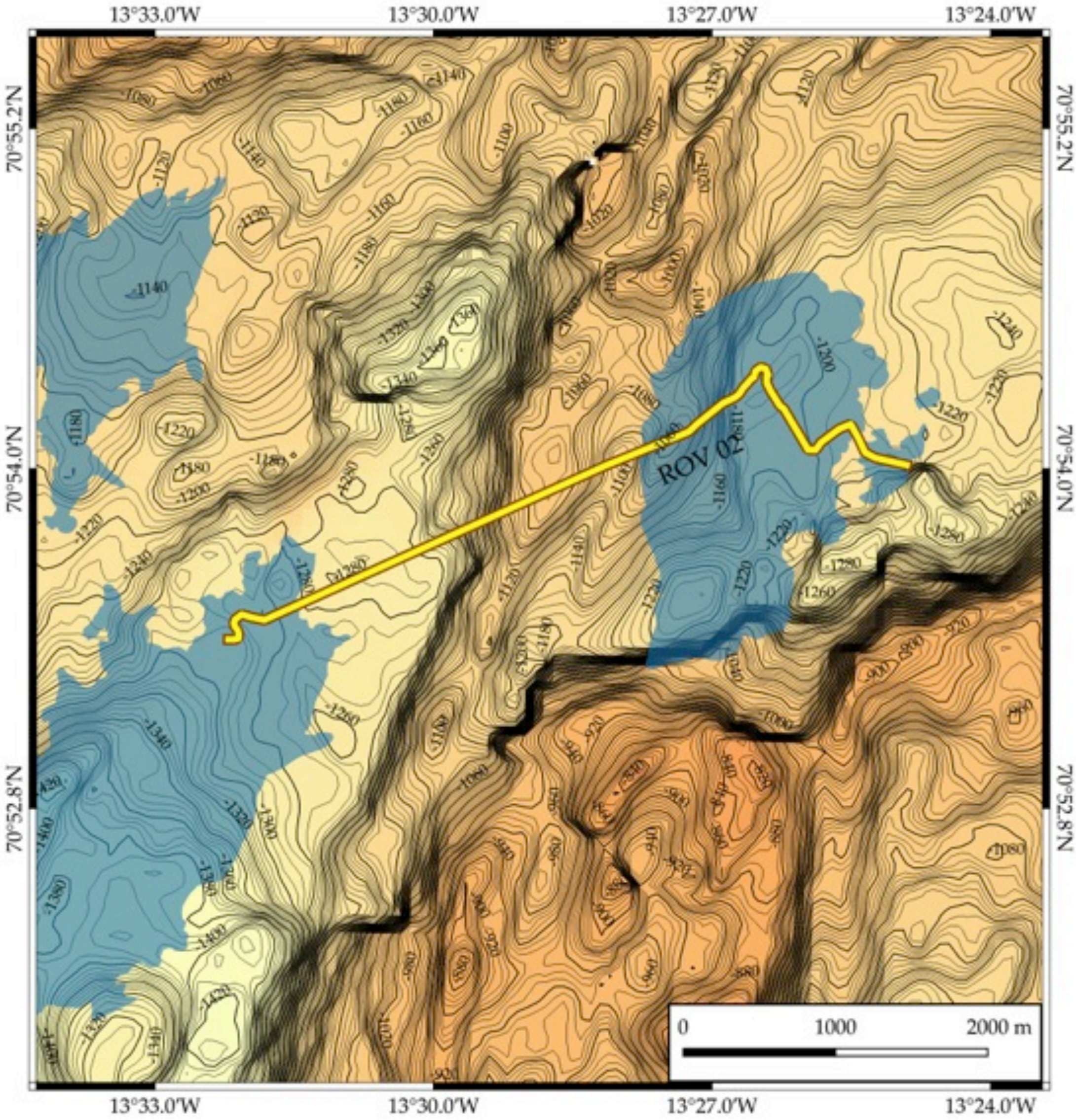

Notes:	Older more sedimented pillowed and lobate flows observed in east, younger, hackly and whorly sheet flows in west

Station Number:	315-ROV		
Cruise Number:	POS502	**Equipment:**	DeepSurveyCam
Date:	21.07.2016		
Time in Water:	13:45	**Issues:**	No navigation from USBL, mission aborted after a few minutes
Time on Bottom:	14:21		
Time off Bottom:	17:00		
Time out of Water:	17:20		
Total Dive Time:	03:36		
Total Bottom Time:	02:39		
Distance Covered:	0.4 km	**Lat/Lon**	71° 16.05 −012° 43.86

Dive Map:

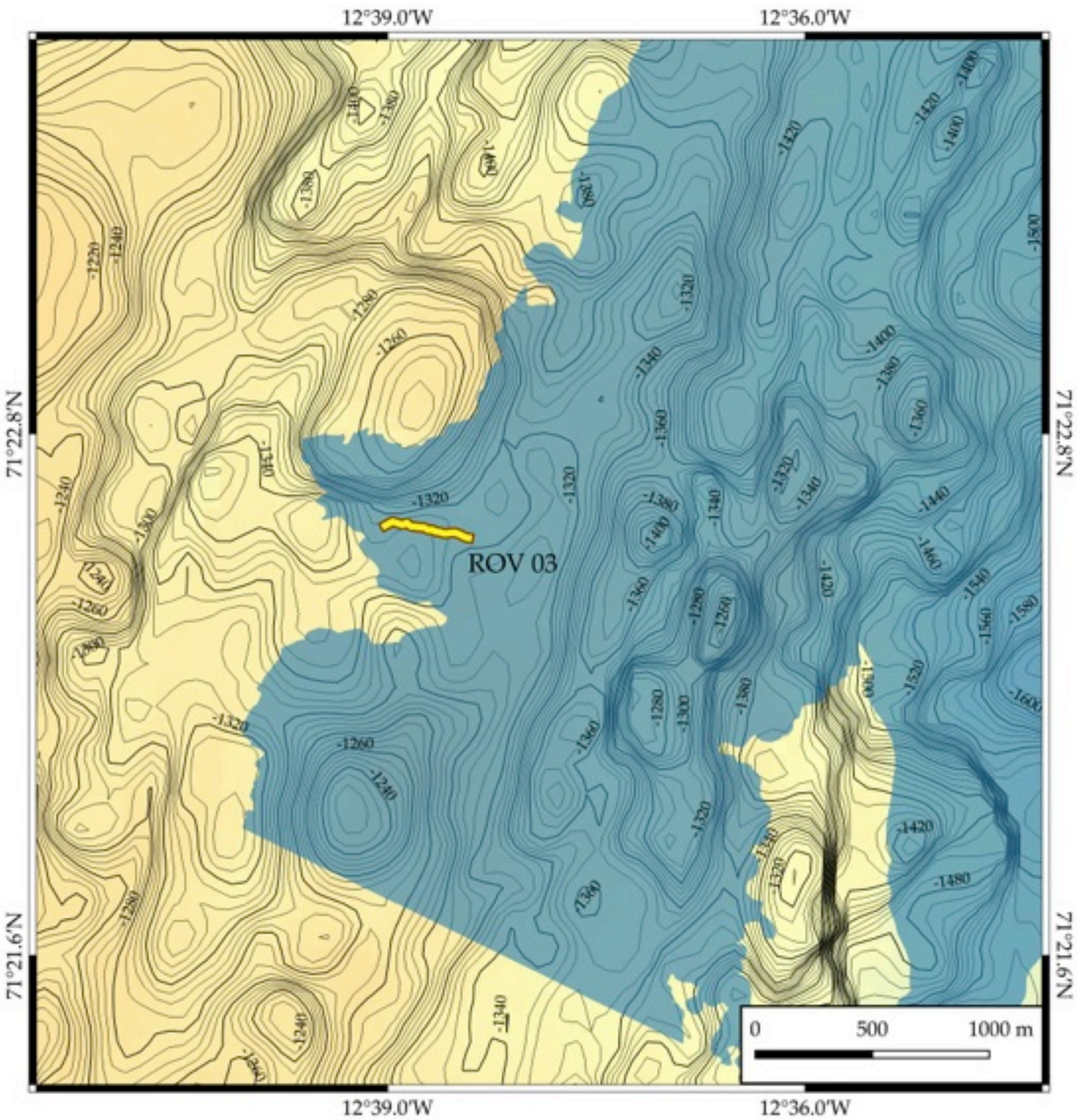

Notes:	Pillow lavas with a thin dusting of sediment observed. Slightly older than 298-ROV.

Station Number:	333-ROV			
Cruise Number:	POS502	**Equipment:**	DeepSurveyCam	
Date:	23.07.2016			
Time in Water:	14:04	**Issues:**	No navigation from USBL, short test mission. Suspect on transponder malfunctioning.	
Time on Bottom:	14:19			
Time off Bottom:	16:09			
Time out of Water:	16:22			
Total Dive Time:	02:18			
Total Bottom Time:	01:50			
Distance Covered:	1.1 km	**Lat/Lon**	70° 57.04	-013° 03.42

Dive Map:

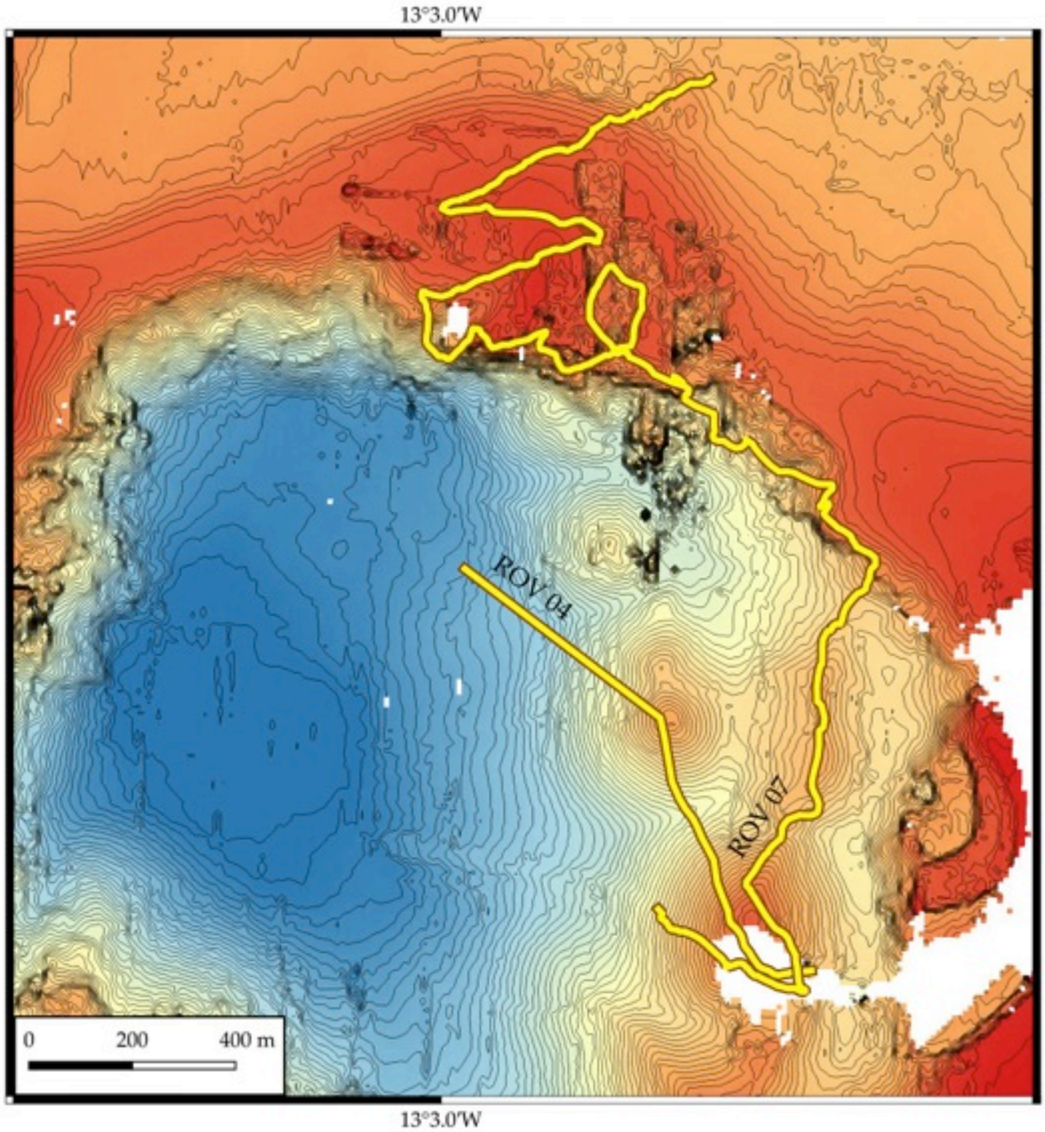

Notes:	Young, vesicular, dark volcanic material. Cones younger than crater floor. Evidence for hydrothermal activity.

Station Number: 335-ROV

Cruise Number:	POS502	**Equipment:**	DeepSurveyCam	
Date:	24.07.2016			
Time in Water:	08:55	**Issues:**	USBL navigation back with one transponder	
Time on Bottom:	09:19			
Time off Bottom:	13:31			
Time out of Water:	13:56			
Total Dive Time:	05:01			
Total Bottom Time:	04:12			
Distance Covered:	4.2 km	**Lat/Lon**	71° 12.03	-012° 52.33

Dive Map:

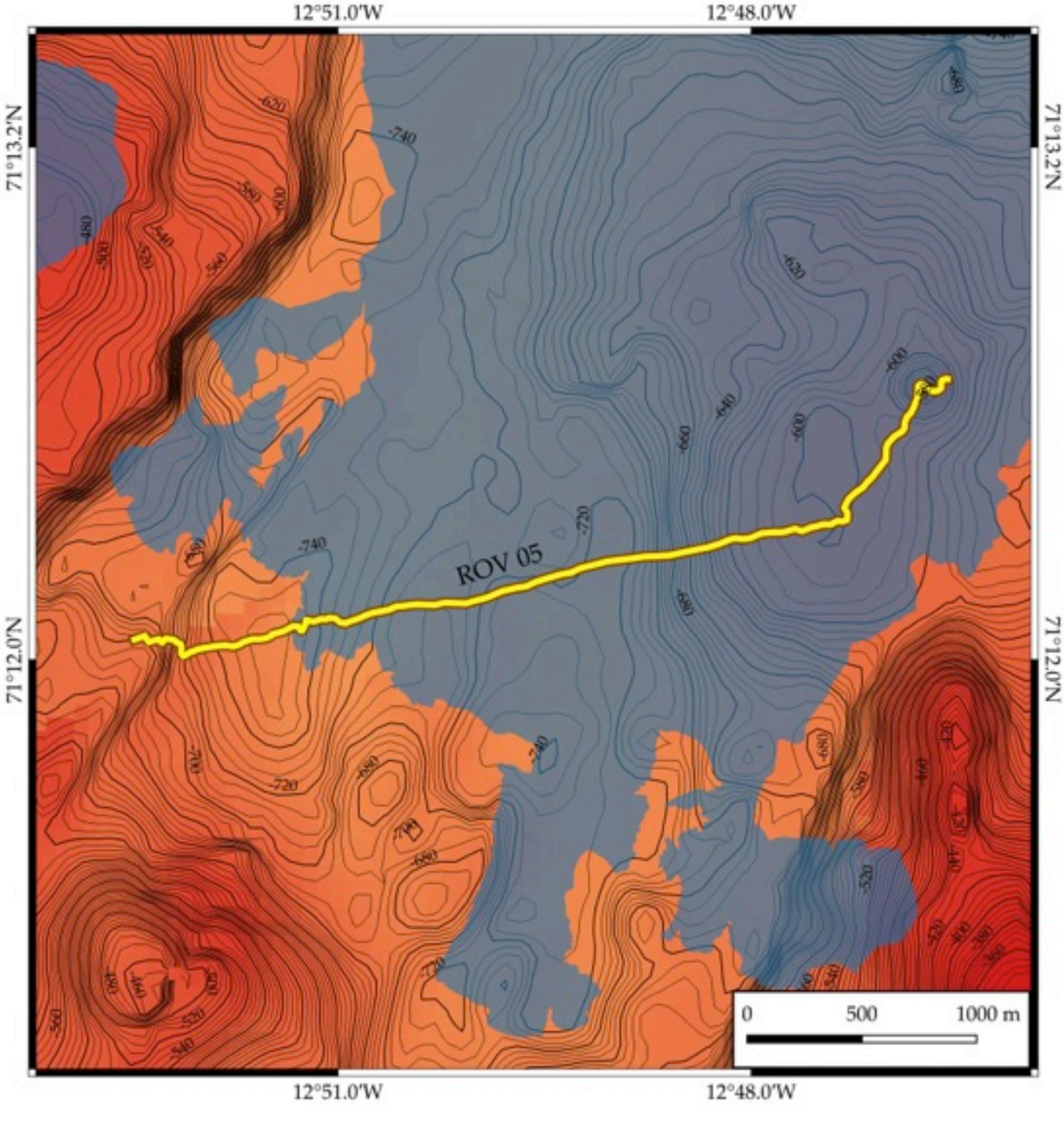

Notes:	Young looking, large proportion sheet flows. Crater young and hydrothermal activity detected between crater and pillow mound.

Station Number:	341-ROV			
Cruise Number:	POS502	**Equipment:**	DeepSurveyCam	
Date:	25.07.2016			
Time in Water:	12:27	**Issues:**	Tether severely twisted on bottom. Mission immediately aborted.	
Time on Bottom:	13:13			
Time off Bottom:	13:55			
Time out of Water:	14:48			
Total Dive Time:	02:21			
Total Bottom Time:	00:42			
Distance Covered:	x	**Lat/Lon**	71° 22.57	−012° 38.90
Dive Map:				
Notes:	Dive aborted. Young pillows briefly seen.			

Station Number:	346-ROV		
Cruise Number:	POS502	**Equipment:**	DeepSurveyCam
Date:	26.07.2016		
Time in Water:	08:34	**Issues:**	Tether damaged during mission but did not effect operations
Time on Bottom:	09:03		
Time off Bottom:	14:50		
Time out of Water:	15:02		
Total Dive Time:	06:28		
Total Bottom Time:	05:46		
Distance Covered:	4.7 km	**Lat/Lon**	70° 56.73 / -013° 3.25

Dive Map:

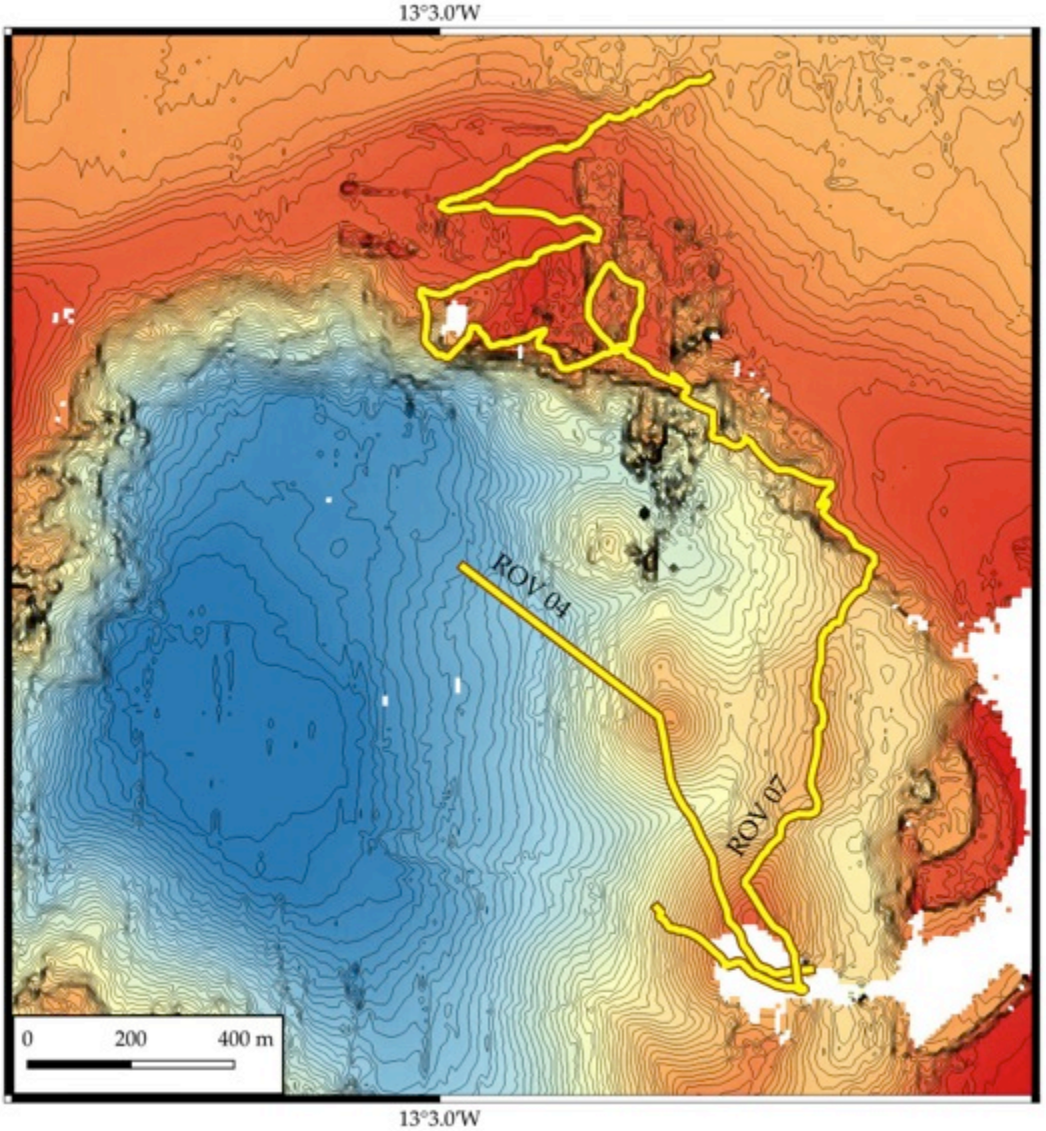

Notes:	Much young looking vesicular material. Hydrothermal activity detected. Everything covered in ash layer that postdates caldera.

7. Volcanic Wax Corer (VSR) Sampling and Dredging (Elkins, Devey)

7.1 Summary

The primary goals of sampling on this expedition were to ground-truth sidescan sonar measurements conducted on the previous POS436 cruise with direct sampling of seafloor material, and to follow up on that sampling with geochemical analysis to assess whether adjacent stations sampled a single large lava flow or distinct mappable units. Sampling was mostly conducted by wax coring (Fig. 1. And Fig. 2), plus two additional dredge stations conducted with the chain dredge to retrieve larger rock samples and complement new bathymetric mapping efforts.

Overall, material retrieved by the wax core matched expectations for fresh, altered, or sedimented lava flows based on sidescan analysis and predictions. Two stations retrieved only mud, which was not saved for chemical analysis. Only one station (VSR-22) failed to retrieve any material; that station was then repeated at higher descending speed and did succeed on the second try (VSR-23). Most of the sampling localities hosted fresh lava that appeared bright and reflective on sidescan, and fresh glassy rock chips were retrieved by the wax corer, frequently including large chips up to a centimetre in diameter. Areas that appeared less bright on sidescan overall resulted in more weathered looking rock material, typically with some mud. Very dark sidescan areas produced only mud. We found this method to be particularly successful for ground-truthing efforts of this type, due to the fast nature of the sampling compared with other methods (e.g., dredging).

The newly mapped off-axis area east of the Eggvin seamount was not sampled in 2012, so we supplemented our sampling efforts with a dredge attempt in that region; that dredge retrieved more altered and weathered basalt that appeared to have been eroded from a relatively old volcanic source, as well as a number of highly rounded and weathered rocks we interpreted to be glacial dropstones. We interpreted this result to indicate that eruptions along the volcanic terrain to the east of Eggvin predate the last glacial maximum.

Our final dredging effort was conducted in the Eggvin seamount steep-walled summit crater, in an attempt to replicate the retrieval of popping rocks in 2012 for further chemical analysis. Although less vigorous, the highly vesicular volcanic cinders retrieved did pop after retrieval. In an attempt to preserve the popping rock samples for analysis of vesicle gases, we vacuum-sealed four samples to reduce air contamination. Each sample was treated differently (one was not rinsed to remove seawater; one was rinsed and bagged immediately; and the remaining two were dried in the drying oven and sealed later), in an attempt to provide a means of correction for any air contamination that may have occurred after removal from the seafloor. Other fresh popping rocks from the summit crater dredge were archived for future research efforts.

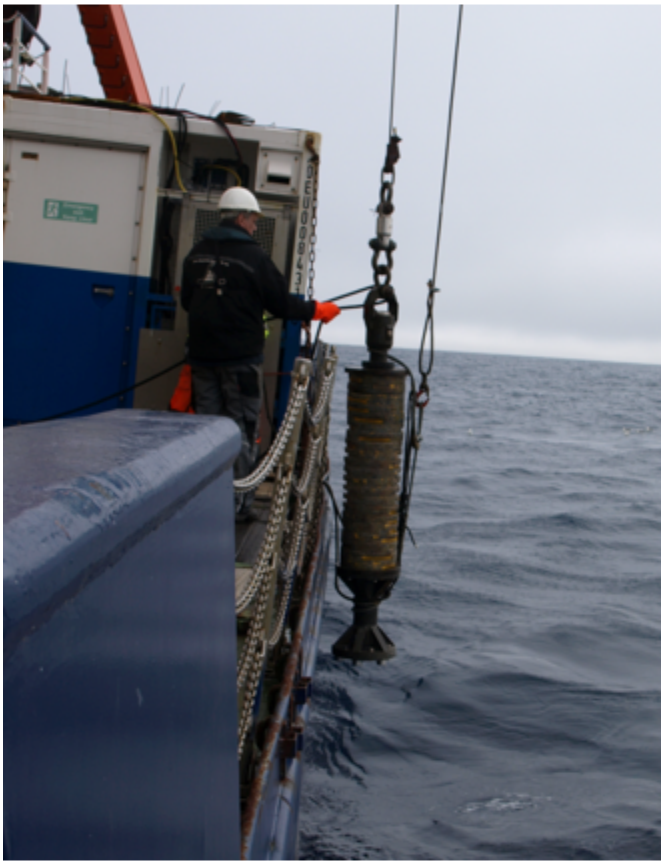

Fig 7.1: The Volcanic Wax Corer and weight being deployed over the side of the ship

Fig. 7.2: The head after a successful deployment showing glass chips caught in the wax filled cups

7.2 Location Maps

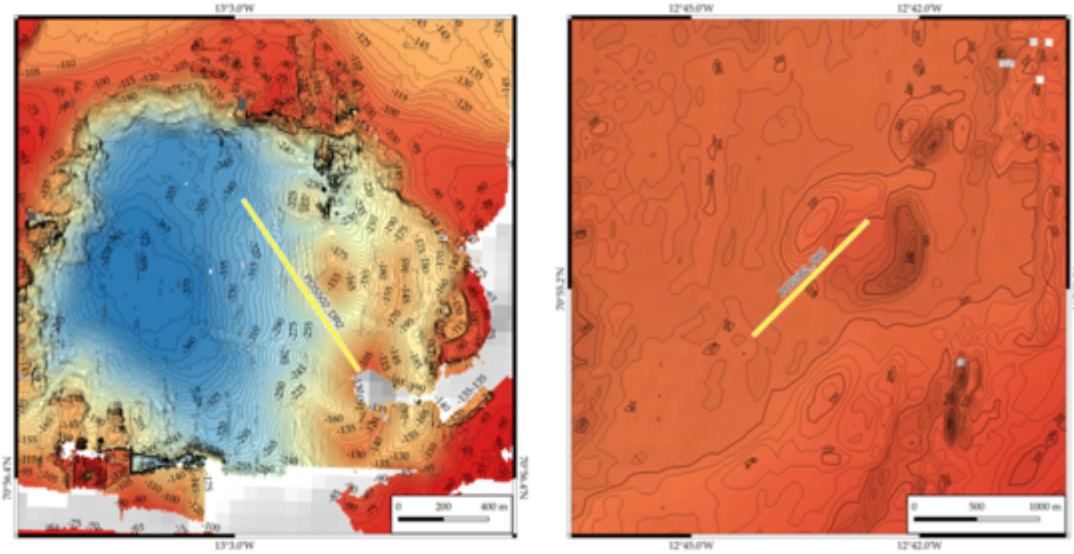

Fig. 7.3 Dredge locations on ship bathymetry

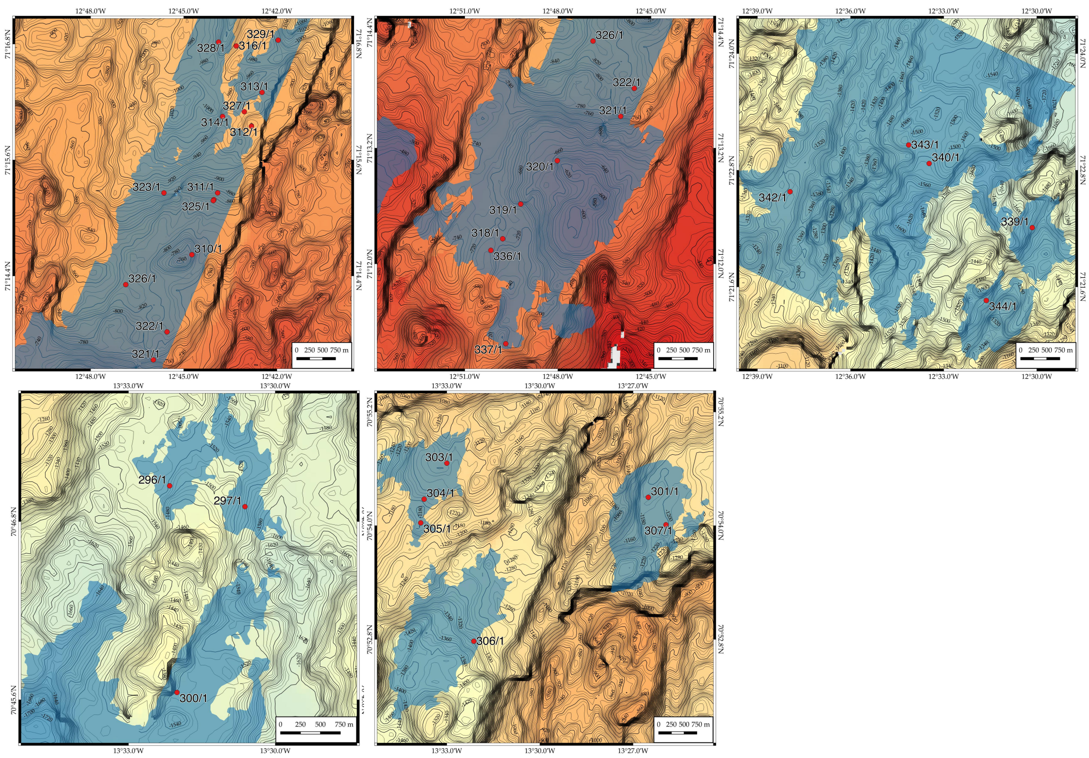

Fig. 7.4 Volcanic Wax Corer locations superimposed on the ship bathymetry and lava flow field outlines mapped from the POS436 AUV Abyss sidescan sonar data

7.3 POS-502 Wax corer station log

Date	Ship Station Number	Corer Station	Latitude	Longitude	Mesured depth (m)	MAPR on cable? Y/N	Start time (UTC)	Time on bottom (UTC)	Cable length at bottom	End time (UTC)	Material recovered?	Number of cups successful	Notes
18.07.16	296	VSR-01	70°47.03N	13°32.16´W	1550	N	9:38	10:05	1552	10:32	yes - glass chips	3	
18.07.16	297	VSR-02	70°46.9´N	13°30.62´W	1555	N	10:50	11:15	1551	11:37	yes - glass chips	3	4 cups in bag - one new cup contaminated with a jumping chip while extracting a used cup
19.07.16	300	VSR-03	70°45.65´N	13°32.01´W	1550	N	13:32	14:00	1570	14:23	yes - glass chips	6+	removed all 7 cups to clean holders
19.07.16	301	VSR-04	70°54.30´N	13°26.51´W	1223	N	15:39	16:00	1228		mud	0	no sample taken, then winch broke
20.07.16	303	VSR-05	70°54.66´N	13°33.00´W	1140	N	8:05	8:25	1172		yes - glass chips	2	
20.07.16	304	VSR-06	70°54.28´N	13°33.73´W	1160	N	8:51	9:11	1189	9:28	yes - glass chips	4	
20.07.16	305	VSR-07	70°54.03´N	13°33.84´W	1204	N	9:39	9:58	1201		yes - glass chips	7	
20.07.16	306	VSR-08	70°52.78´N	13°32.14´W	1332	N	10:37	11:00	1326		yes - glass chips	3	
20.07.16	307	VSR-09	70°54.01´N	13°25.93´W	1234	N	11:48	12:07	1229		yes - glass chips	4	some sed.
21.07.16	310	VSR-10	71°14.62´N	12°44.74´W	800	N	9:33	9:48	794	9:58	yes - glass	3	1 full, 2 traces
21.07.16	311	VSR-11	71°15.26´N	12°43.91´W	893	N	10:19	10:33	897		yes - small glass chips	1	Traces of mud
21.07.16	312	VSR-12	71°15.95´N	12°42.82´W	1004	N	11:04	11:22	999	11:34	Mud	0	Did not save
21.07.16	313	VSR-13	71°16.30´N	12°42.48´W	983	N	12:00	12:16	977	12:28	Yes - chips in cups, rock on side!	6	Rock had fresh glass on both sides, no vesicles or phenos visible
21.07.16	314	VSR-14	71°16.05´N	12°43.75´W	1017	N	12:47	13:04	1011		Yes - one small piece	1	
21.07.16	316	VSR-15	71°16.78´N	12°43.31´W	1040	N	17:34	17:53	1035		Yes - glass	3	One large (2cm) piece
22.07.16	318	VSR-16	71°12.26´N	12°49.78´W	734	N	7:56	8:08	728	8:18	yes - small glass & rock chips	1	2nd cup with mud also taken
22.07.16	319	VSR-17	71°12.62´N	12°49.20´W	740	N	8:37	8:53	739		yes, one larger chip. Looks old	5	
22.07.16	320	VSR-18	71°13.07´N	12°48.02´W	686	N	9:26	9:35	680		yes, glass chips looking fresh	3	
22.07.16	321	VSR-19	71°13.53´N	12°45.98´W	778	N	10:06	10:20	784		yes - cups full	5	
22.07.16	322	VSR-20	71°13.82´N	12°45.54´W	819	N	10:44	10:58	816		yes - glass chips	3	
22.07.16	323	VSR-21	71°15.26´N	12°45.64´W	926	N	11:59	12:14	930		yes - glass with some mud	2	
22.07.16	324	VSR-22	71°15.19´N	12°44.03´W	882	N	12:42	12:59	876		no	0	redo
22.07.16	325	VSR-23	71°15.18´N	12°44.05´W	884	N	13:17	13:33	874		yes - glass with mud	6	repeat of last station
22.07.16	326	VSR-24	71°14.31´N	12°46.87´W	884	N	14:11	14:26	880		yes - v. fresh glass, little sediment	4	
22.07.16	327	VSR-25	71°16.10´N	12°43.05´W	1002	N	15:12	15:29	993		yes - glass chips	1	
22.07.16	328	VSR-26	71°16.82´N	12°43.88´W	1015	N	16:13	16:33	1009		yes - glass	5	
22.07.16	329	VSR-27	71°16.84´N	12°41.96´W	1000	N	17:07	17:22	985	17:35	mud, one rock fragment	1	
24.07.16	336	VSR-28	71°12.14´N	12°50.16´W	738	N	14:22	14:36	728		yes - fresh glass	7	
24.07.16	337	VSR-29	71°11.17´N	12°49.68´W	720	N	15:09	15:20	715		yes - mud with glass	0	saved scraped-off mud
25.07.16	339	VSR-30	71º22.21'N	12º30.15'W	1597	N	9:08	9:35	1607		yes - glass, some mud	3	
25.07.16	340	VSR-31	71º22.865'N	12º33.471'W	1598	N	10:22	10:47	1598		yes - mud, trace glass chips	2	
25.07.16	342	VSR-32	71º22.58'N	12º37.94'W	1359	N	15:03	15:26	1358		mud? + a sample from edge of corer	2	
25.07.16	343	VSR-33	71º23.057'N	12º37.94'W	1480	N	16:03	16:26	1508		glass chips, trace mud	4	
25.07.16	344	VSR-34	71º21.461'N	12º31.635'W	1513	N	17:14	17:38	1520		glass chips, trace mud	4	

7.3 POS-502 Dredge station log

Station Area	Date	Start					Stop					Sample descriptions and samples taken
		Time (UTC)	Latitude (ºN)	Longitude (ºW)	Depth (m)	Wire length	Time (UTC)	Latitude (ºN)	Longitude (ºW)	Depth (m)	Wire length	
331DS (East of Eggvin)	23.07.16	8:15	70º55.006'	12º44.162'	680	679	9:45	70º55.486'	12º42.700'	629	628	Few rocks and mud; altered basalt and small dropstones **-B (biology):** Mud; to GEOMAR (in freezer) **-1:** weathered basalt with red coating, some glass, no vesicles or visible phenocrysts, rounded, 9x4x4 cm; to GEOMAR **-2:** Weathered unknown rock (maybe diabase?), some red coating, no vesicles, white phenocrysts (plagioclase?), very rounded, likely dropstone, 9.5x5x14 cm; to GEOMAR **-3:** weathered basalt, maybe old glass rind with some red alteration, 5x4x1 cm; to GEOMAR. **-4:** Assorted small dropstones.
332DS (Eggvin crater) Steep-walled crater with small cones; Dredged over two cones	23.07.16	12:04	70º57.06'	13º02.93'	327	337	13:18	70º56.66'	13º02.10'	109	118	Half full dredge with cinders/popping rocks Crinoids, mussels, scallops **-1:** fresh popping rock, crumbly, very vesicular, glassy 11x9x9 cm; vacuum-sealed with no rinsing; to UNL **-2:** similar to first, 17x11x9 cm; vacuum-sealed after rinsing; to UNL **-3:** similar to first, 10x10x9 cm; dried for one hour, then vacuum-sealed; to UNL **-4:** similar to first, 13x11x9 cm; dried for two hours, then vacuum-sealed; to UNL **-5:** similar to first, 16x10x10 cm; to GEOMAR **-6:** similar to first, 9x11x9 cm; to GEOMAR **-7:** similar to first, 9x8x9 cm; to GEOMAR **-Extras:** similar, assorted larger samples, unnumbered; to GEOMAR

8. Photogrammetry (Kwasnitschka)

A high-resolution SLR stills camera was carried on ROV PHOCA (Figure 1) in order to conduct photogrammetric surveys of the sea floor for later structural, volcanological and habitat studies in addition to seafloor reflectivity studies in combination with sidescan backscatter quantification.

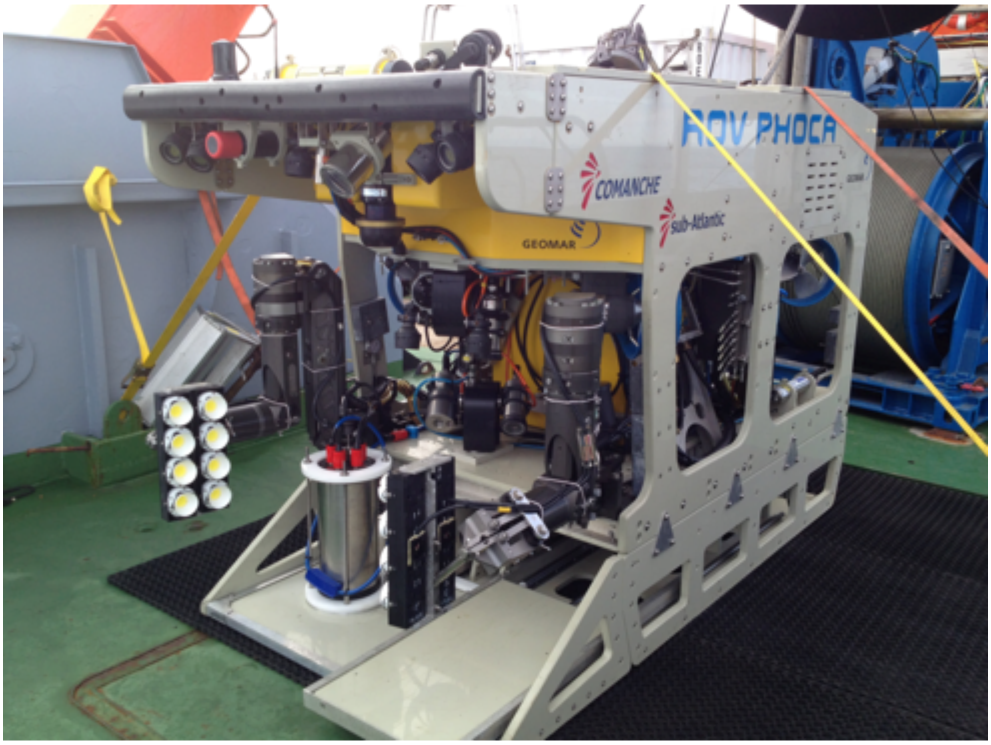

Figure 8.1 ROV Phoca with the DeepSurveyCam mounted on the front porch.

A CANON Eos 6D SLR of 20MP resolution with a 15mm fisheye lens (CANON 8-15mm f4.5 zoom) was employed as part of the DeepSurveyCam package described in [*Kwasnitschka et al.*, 2016]. This system was developed for the AUV Abyss and uses a high power LED strobe. Of the three strobe arrays normally employed only two were carried on either manipulator of the ROV while the third remained unused. Thus it was possible to precisely adapt the illumination pattern to the requirements of the terrain. The camera was mounted on the starboard front porch facing vertically downward, oriented in landscape mode relative to the direction of travel (Fig. 8.1). Camera orientation was logged inside the camera housing and will be fused with other navigation information.

A total of seven surveys were conducted. Table 8.1 gives the statistics of each dive. After the first dive, it was decided that the cadence could be lowered from 1 fps to 1/2.5 fps and this value was maintained. This not only reduced wear on the equipment but also allowed recording the imagery in 12 bit Canon RAW format.

Table 8.1 Statistics of photogrammetric coverage

Station/Dive	Frames	Format
298ROV01	10057	jpg
308ROV02	5198	jpg/raw
315ROV03	1249	jpg/raw
333ROV04	2416	jpg/raw
335ROV05	5853	jpg/raw
341ROV06	86	jpg/raw
346ROV07	8120	jpg/raw

Visibility varied between sites due to varying particulate matter in the water column, so an optimum altitude of four meters was aimed for. Useful results were gathered at up to 6 m altitude while the continuity of the reconstruction could still be maintained at 8 m altitude. At an across track field of view of about 160°, this resulted in a useful track width of about 15m limited by scattering and absorption. Minimum altitude was around 2 m dictated by the amount of overlap between each image (Figure 8.2).

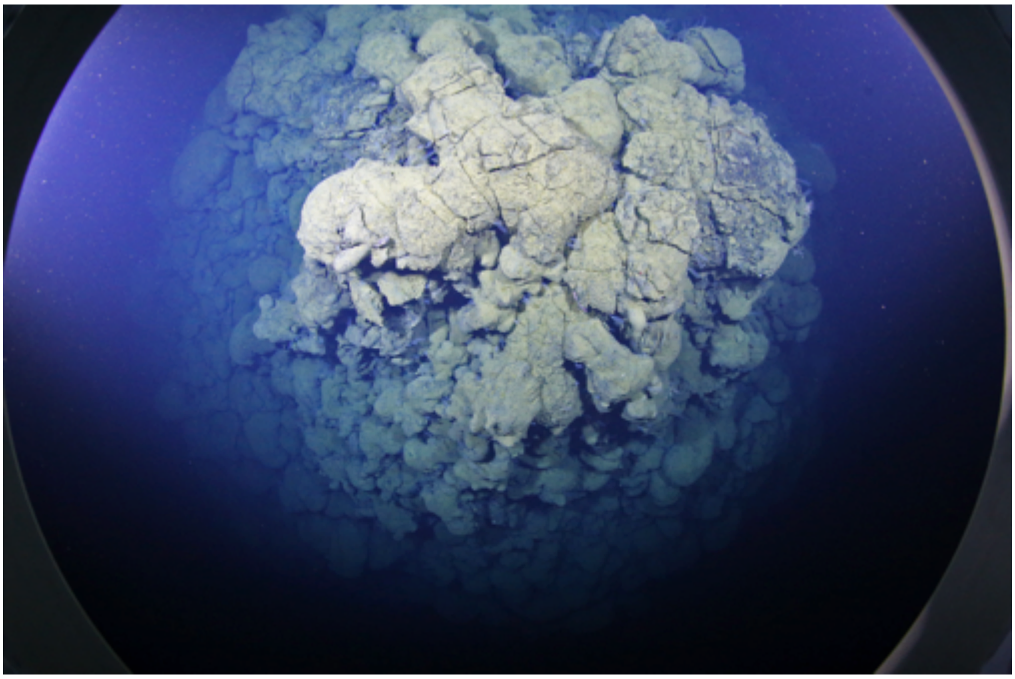

Figure 8.2 A frame of dive 335ROV05, foreground 4 m away, background 10 m away.

Processing on shore will involve the correlation and cross-referencing of USBL and DVL navigation records, which then serve as a first order pose estimation to initialize the photogrammetric reconstruction and, together with sidescan and multibeam maps, form the basis for georeferencing of the reconstructions. Photogrammetric reconstructions will be done using the Agisoft Photoscan Pro software as detailed in [*Kwasnitschka et al.*, 2012]. Preliminary tests were conducted while aboard on the data of dive X and Y in order to verify sufficient overlap along track (figure 8.3). The full reconstruction will be done ashore due to limited computing power.

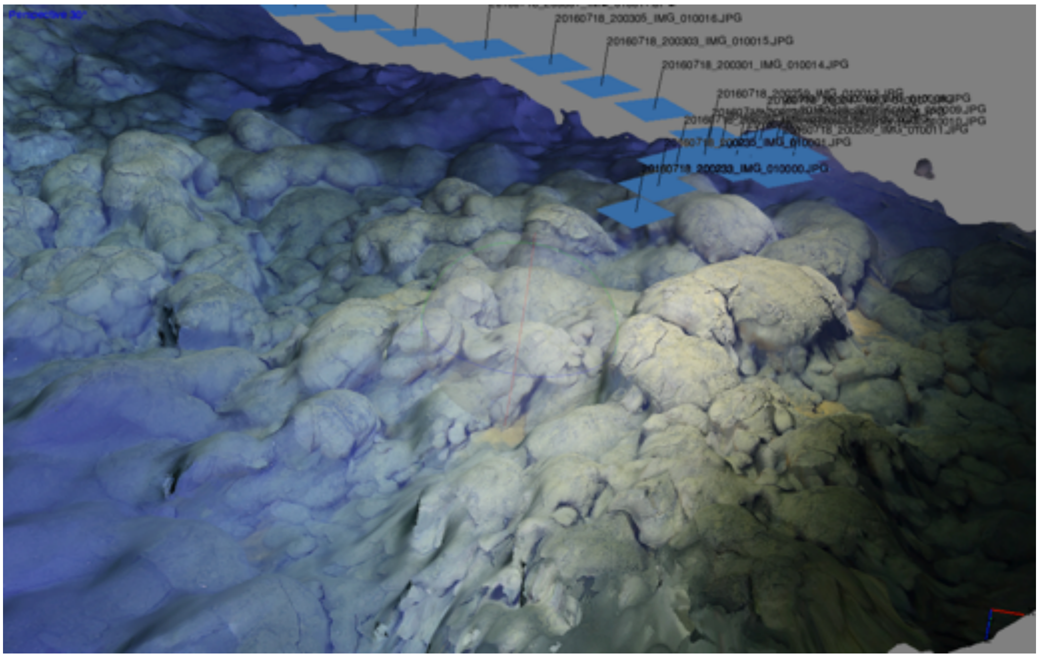

Figure 8.3 Test reconstruction of a pillow field of dive 298ROV01. Blue sprites represent the camera poses relative to the terrain.

9. MAPR Deployments (Devey)

MAPR (Baker and Millburn, 1997) are autonomous pressure, temperature, turbidity and oxidation/reduction potential (ORP) recorders produced and maintained by the NOAA PMEL lab in Seattle. Two MAPR (numbers 66 and 73) were on board POS-502, for all but one deployment MAPR 73 was used. Operational constraints (shallow station depths and hence short winch times) meant that we did not deploy MAPR on the wax-corer sampling stations (such a deployment would, on average, have extended the station time by an estimated 10-20%) but we did attach a MAPR to the ROV on all deployments. In view of the lack of high-temperature venting signals seen on the North Kolbeinsey Ridge in 2012 during POS-436, the near-bottom deployment on the ROV is probably a more efficient way to perform hydrothermal surveys on this ridge. Use on a ROV does, however, mean that spurious turbidity signals can often be generated when propeller wash stirs up sediment. For this reason we confined our hydrothermal interpretations to the OPR sensor.

Details of the individual dives are given below:

<u>298_ROV</u>

The plot of delta ORP (mV/s) vs. time for the dive is shown on Fig. 9.1. For details of the dive track see the ROV reports in section 6. As the sensor is prone to drift and it is the rate of change in ORP with time, which is related to signal strength, we used this as a more useful value than absolute ORP. According to recently published work by Baker et al. (2016), a delta-ORP signal > 0.02mV/sec. is a significant anomaly.

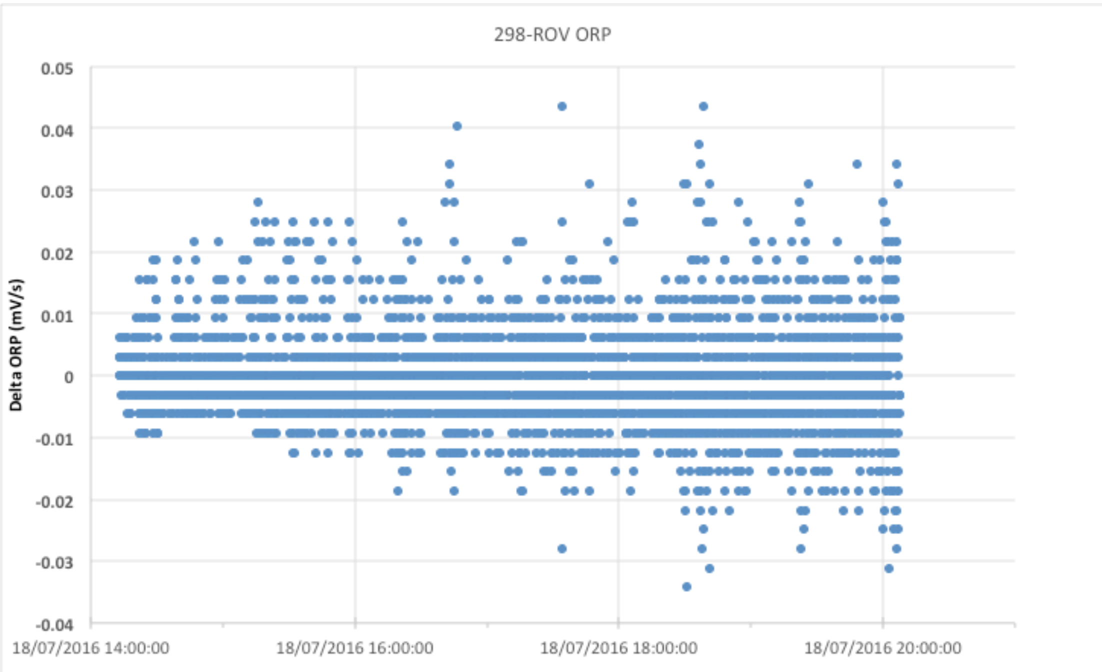

Fig. 9.1: Delta ORP vs. date-time during the dive.

Apparently randomly spaced and very small anomalies along the profile are not clearly correlated with any particular features on the seafloor, the vast majority of values lie below the 0.02mV/s threshold.

<u>308-ROV</u>

The MAPR results from 308-ROV (Fig. 9.2) are also mainly below the anomaly threshold. Single values rising as high as 0.04mV/s are not obviously correlated with notable seafloor features.

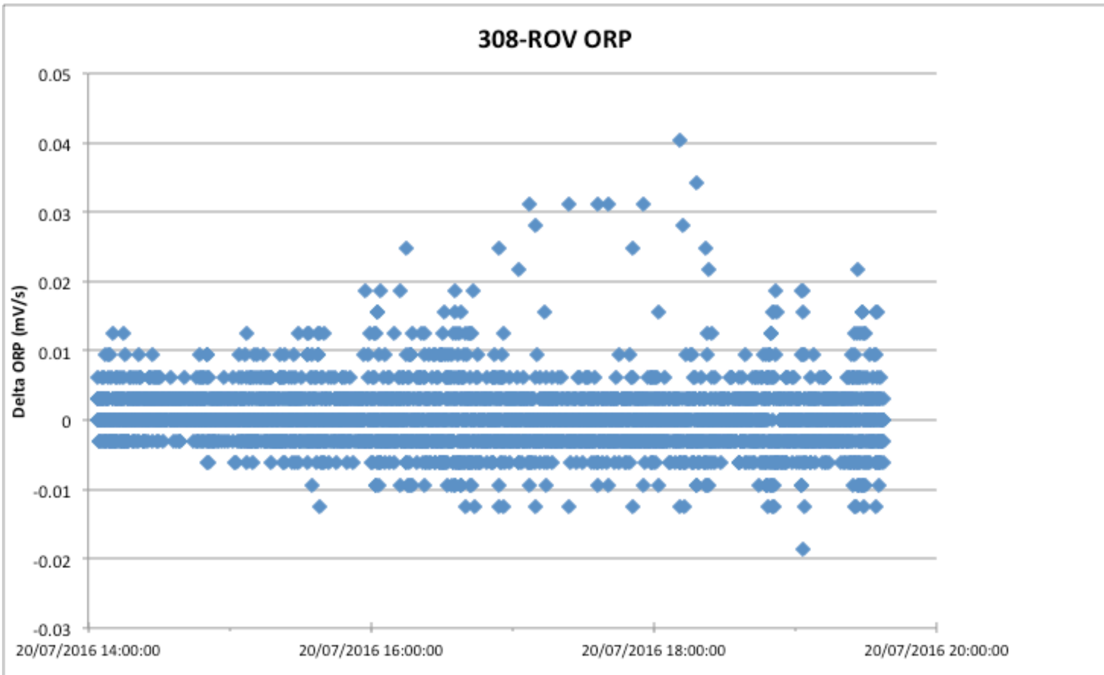

Fig. 9.2: The delta-ORP values plotted against time during dive 308-ROV

<u>315-ROV</u>

Dive 315-ROV only descended to the bottom and then had to return due to technical problems. The MAPR showed no anomalies on this effective vertical cast (Fig. 9.3).

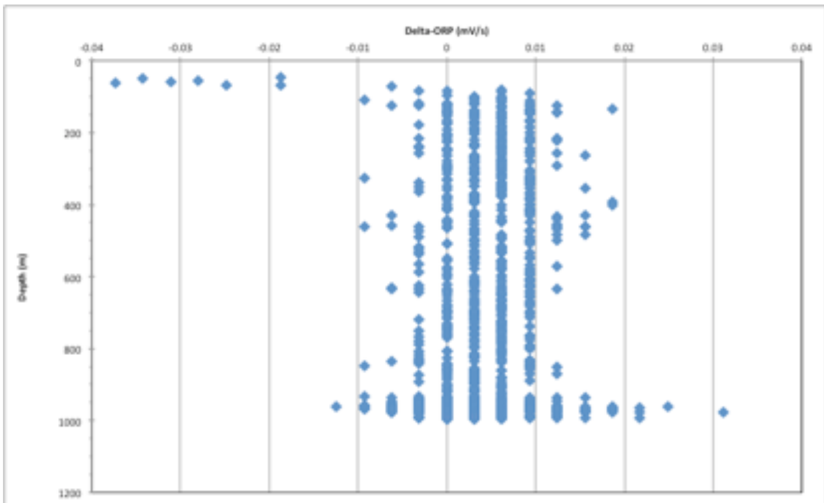

Fig. 9.3: The delta-ORP profile from dive 315-ROV plotted as a vertical profile

333-ROV

Most of the MAPR data from dive 333-ROV show no anomalies. But at around 15:25 a large anomaly (0.08 mV/s) is seen in delta-ORP (Fig. 9.4). This anomaly coincided with the approach to a yellow-stained block on the seafloor. Following this, several other similar blocks were seen, these too often associated with slight ORP-anomalies although none as strong as that at 15:25.

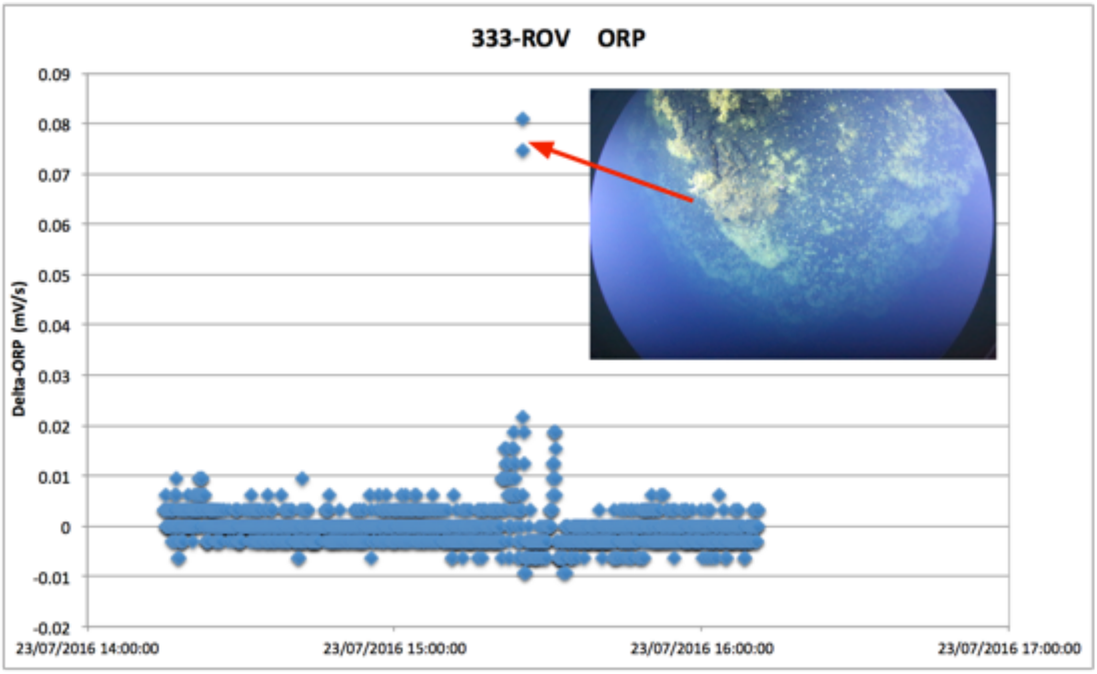

Fig. 9.4: The ORP-anomaly on 333-ROV was clearly associated with strong iron-staining on the seafloor. Close examination of the photo shows that this iron-stained area is the only hard substrate devoid of feathery crinoids.

335-ROV

This dive showed a generally higher degree of variation in the delta-ORP values and two regions with pronounced anomalies (Fig. 9.5). The first of these was in an extensive area showing signs of the accumulation of iron-hydroxide sediments, presumably a former hydrothermal mound. Evidence from the photogrammetry suggests we skirted this mound on its eastern side. A much larger anomaly was seen on the summit of the final hill during the dive - these numerous large anomalies (reaching up to 0.18mV/s) were associated with small clumps of red/pink anemones on the seafloor. These anemones appeared only in this area and were highly concentrated at a few places. We assume they are the sites of low-temperature venting, although no direct evidence (e.g. shimmering water) was seen.

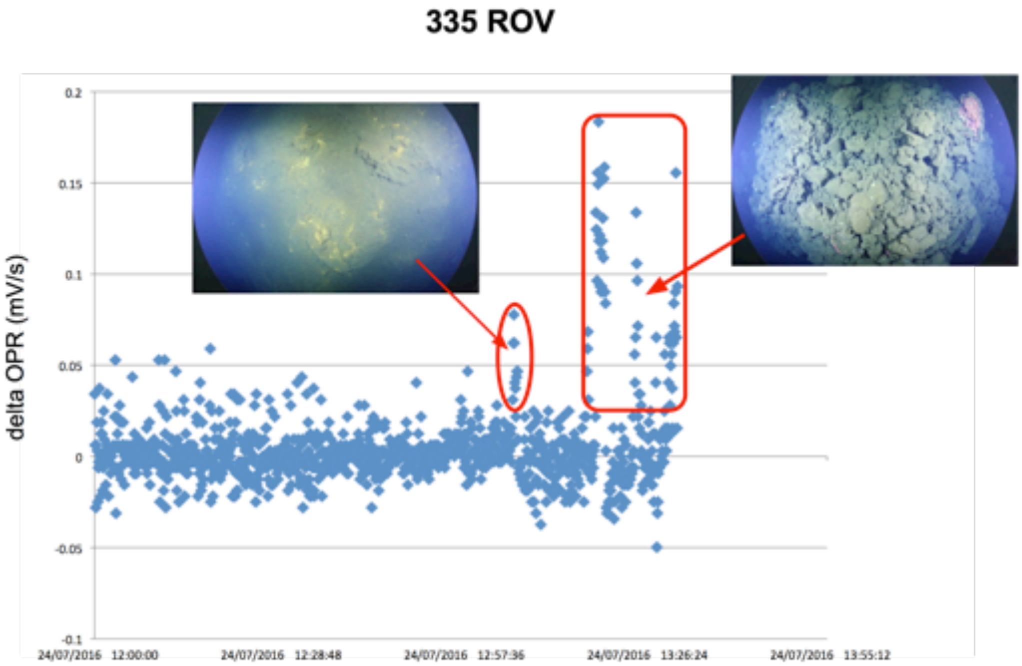

Fig. 9.5: Plot of delta-ORP vs. time. Note the generally higher variability in the values compared to previous dives and the clear association of some ORP-anomalies with seafloor features.

<u>341-ROV</u>

This short dive showed no ORP-anomalies (see Fig. 9.6)

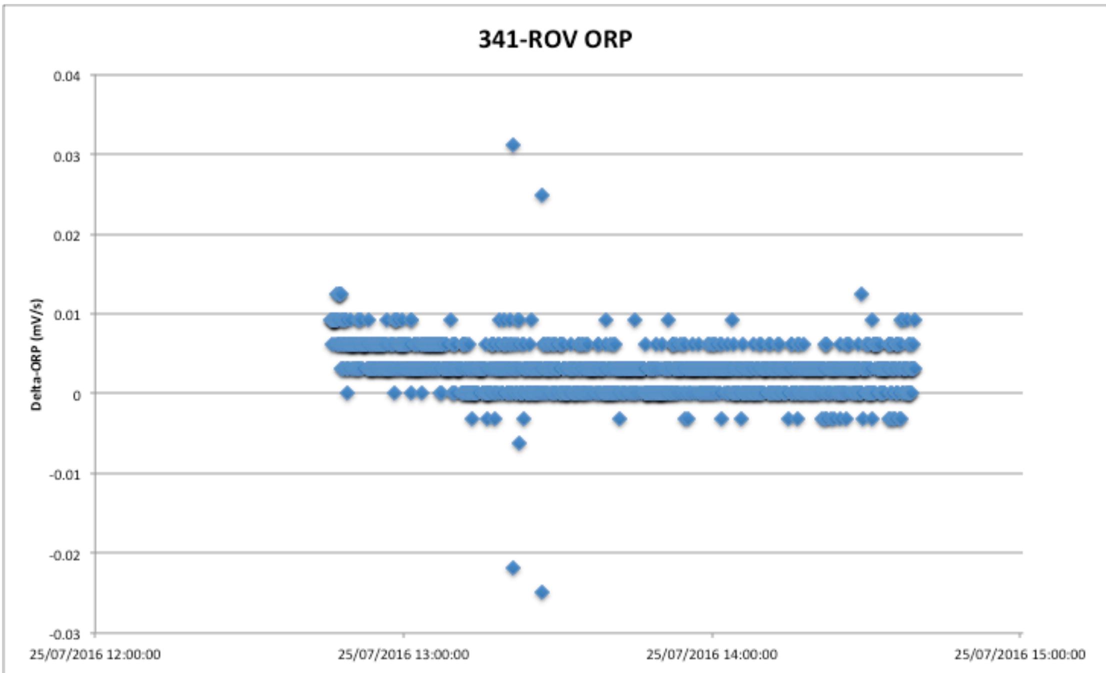

Fig. 9.6: The ORP-values during dive 341-ROV.

346-ROV

Despite showing some evidence of past hydrothermal activity (isolated eroded chimneys, some orange-stained boulders) on the seafloor, the ORP-sensor showed no anomalies during the dive (see Fig. 9.7)

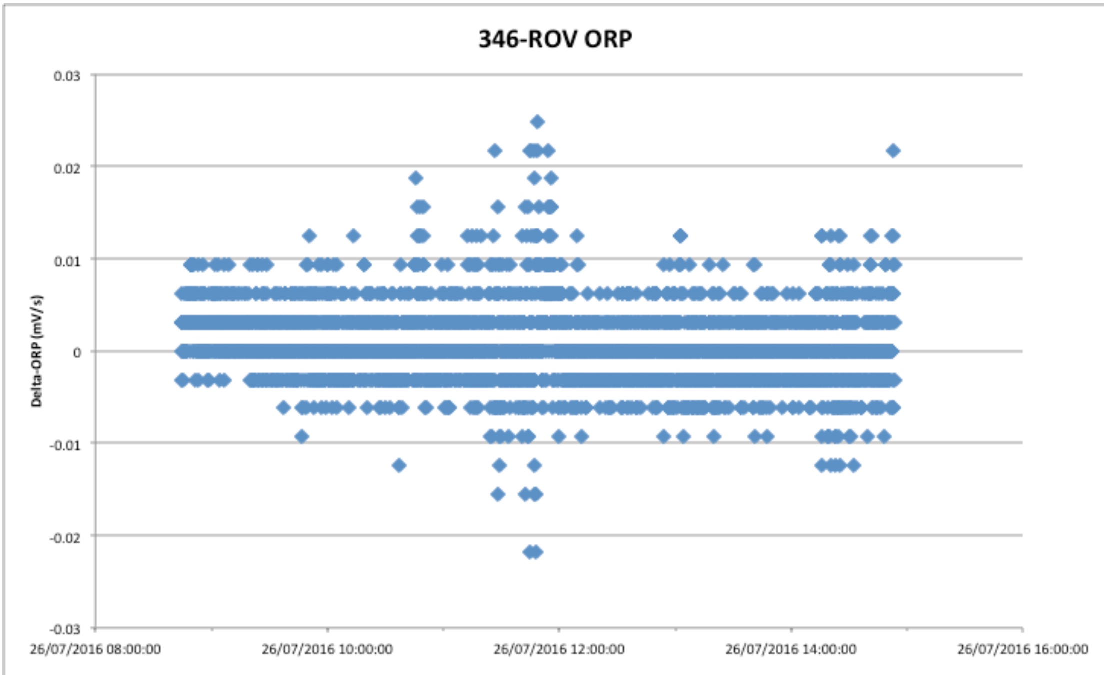

Fig. 9.7: The delta-ORP values during dive 346-ROV.

10. Literature

Baker, E.T. and Millburn, H.B., 1997. MAPR: A new instrument for hydrothermal plume mapping. Ridge Events, 8(1): 23-25.

Baker, E.T., Resing, J., Haymon, R.M., Tunnicliffe, V., Lavelle, J.W., Martinez, F., Ferrini, V.L., Walker, S.L. and Nakamura, K., 2016. How many vent fields? New estimates of vent field populations on ocean ridges from precise mapping of hydrothermal discharge locations. Earth Planet. Sci. Lett., 449: 186-196.

Ballard, R.D., and Van Andel, T.H., 1977, Morphology and tectonics of the inner rift valley at lat 36°50'N on the Mid-Atlantic Ridge: Geological Society of America Bulletin, , no. 4, p. 507–530, doi: 10.1130/0016-7606.

Bowles, J., Gee, J.S., Kent, D. V., Perfit, M.R., Soule, S.A., and Fornari, D.J., 2006, Paleointensity applications to timing and extent of eruptive activity, 9°-10°N East Pacific Rise: Geochemistry, Geophysics, Geosystems, v. 7, no. 6, p. n/a–n/a, doi: 10.1029/2005GC001141.

Bryan, W.B., and Moore, J.G., 1977, Compositional variations of young basalts in the Mid-Atlantic Ridge rift valley Compositional variations of young basalts in the Mid-Atlantic Ridge rift valley near lat 36°49'N: Geological Society of America Bulletin, , no. 4, p. 556–570, doi: 10.1130/0016-7606(1977)88<556.

Caress, D.W., Clague, D.A., Paduan, J.B., Martin, J.F., Dreyer, B.M., Chadwick, W.W., Denny, A., Kelley, D.S., 2012. Repeat bathymetric surveys at 1-metre resolu-tion of lava flows erupted at Axial Seamount in April 2011. Nat. Geosci.5 (7), 483–488. http://dx.doi.org/10.1038/ngeo1496.

Devey, C. W., and the scientific team of POS436, 2012, Cruise Report POS436, GEOMAR, 1–56 p.

Duncan, R.A., Hogan, L.G., 1994. Radiometric dating of young MORB using the 40Ar–39Ar incremental heating method. Geophys. Res. Lett.21 (18), 1927–1930. http://dx.doi.org/10.1029/94GL01375

Escartín, J., Soule, S. a., Fornari, D.J., Tivey, M. a., Schouten, H., and Perfit, M.R., 2007, Interplay between faults and lava flows in construction of the upper oceanic crust: The East Pacific Rise crest 9°25′-9°58′N: Geochemistry, Geophysics, Geosystems, v. 8, no. 6, p. n/a–n/a, doi: 10.1029/2006GC001399.

Fox, C.G., Chadwick, W.W., Embley, R.W., 1992. Detection of changes in ridge-crest morphology using repeated multibeam sonar surveys.

Kwasnitschka, T. et al. (2016), DeepSurveyCam—A Deep Ocean Optical Mapping System, *Sensors*, *16*(2), 164, doi:10.3390/s16020164.

Kwasnitschka, T., T. H. Hansteen, C. W. Devey, and S. Kutterolf (2012), Doing Fieldwork on the Seafloor: Photogrammetric Techniques to yield 3D Visual Models from ROV Video, *Computers and Geosciences*, *52*(52), 218–226, doi:10.1016/j.cageo.2012.10.008.

Mendel, V., Sauter, D., Rommevaux-Jestin, C., Patriat, P., Lefebvre, F., and Parson, L.M., 2003, Magmato-tectonic cyclicity at the ultra-slow spreading Southwest Indian Ridge: Evidence from variations of axial volcanic ridge morphology and abyssal hills pattern: Geochemistry, Geophysics, Geosystems, v. 4, no. 5, p. n/a–n/a, doi: 10.1029/2002GC000417.

Mitchell, N.C., 1993, A model for attenuation of backscatter due to sediment accumulations and its application to determine sediment thicknesses with GLORIA sidescan sonar: Journal, v. 98, no. B12, p. 22477–22493.

Mitchell, N.C., 1995a. Characterising the extent of volcanism at the Galapagos Spreading Centre using Deep Tow sediment profiler records. Earth Planet. Sci. Lett.134 (3–4), 459–472. http://dx.doi.org/10.1016/0012-821X(95)00132-V.

Parson, L.M., Murton, B.J., Searle, R.C., Booth, D., Keeton, J., Laughton, A., Mcallister, E., Millard, N., Redbourne, L., Rouse, I., Shor, A., Smith, D., Spencer, S., Summerhayes, C., et al., 1993, En echelon axial volcanic ridges at the Reykjanes Ridge: a life cycle of volcanism and tectonics: Earth and Planetary Science Letters, v. 117, p. 73–87.

Rubin, K.H., and Sinton, J.M., 2007, Inferences on mid-ocean ridge thermal and magmatic structure from MORB compositions: Earth and Planetary Science Letters, v. 260, no. 1-2, p. 257–276, doi: 10.1016/j.epsl.2007.05.035.

Schouten, H., Tivey, M.A., Fornari, D.J., Cochran, J.R., 1999. Central anomaly mag-netization high: constraints on the volcanic construction and architecture of seismic layer 2A at a fast-spreading mid-ocean ridge, the EPR at 9◦30_–50_N. Earth Planet. Sci. Lett.169 (1–2), 37–50. http://dx.doi.org/10.1016/S0012-821X(99)00063-1.

Searle, R.C., Cowie, P.A., Mitchell, N.C., Allerton, S., Macleod, C.J., Escartin, J., Russell, S.M., Slootweg, P.A., and Tanaka, T., 1998, Fault structure and detailed evolution of a slow spreading ridge segment : the Mid-Atlantic Ridge at 298N: Earth and Planetary Science Letters, v. 154, p. 167–183.

Searle, R.C., Murton, B.J., Achenbach, K., LeBas, T., Tivey, M., Yeo, I., Cormier, M.H., Carlut, J., Ferreira, P., Mallows, C., Morris, K., Schroth, N., van Calsteren, P., and Waters, C., 2010, Structure and development of an axial volcanic ridge: Mid-Atlantic Ridge, 45°N: Earth and Planetary Science Letters, v. 299, p. 228–241, doi: 10.1016/j.epsl.2010.09.003.

Sinha, M.C., Constable, S.C., Peirce, C., White, a., Heinson, G., MacGregor, L.M., and Navin, D. a., 1998, Magmatic processes at slow spreading ridges: implications of the RAMESSES experiment at 57° 45′N on the Mid-Atlantic Ridge: Geophysical Journal International, v. 135, no. 3, p. 731–745, doi: 10.1046/j.1365-246X.1998.00704.x.

Smith, D.K., and Cann, J.R., 1990, Hundreds of small volcanoes on the median valley floor of the Mid-Atlantic Ridge: Nature, v. 348, p. 152–155.

Yeo, I. A., Devey, C. W., LeBas, T. P., Augustin, N., & Steinführer, A. (2016). Segment-scale volcanic episodicity: Evidence from the North Kolbeinsey Ridge, Atlantic. *Earth and Planetary Science Letters*, *439*, 81–87. doi:10.1016/j.epsl.2016.01.029

Yeo, I.A., and Searle, R.C., 2013, High-resolution Remotely Operated Vehicle (ROV) mapping of a slow-spreading ridge: Mid-Atlantic Ridge 45°N: Geochemistry, Geophysics, Geosystems, v. 14, no. 6, p. 1693–1702, doi: 10.1002/ggge.20082.